Universality in Ising-like phase transitions of lattices of coupled chaotic maps

Philippe Marcq,[1,*] Hugues Chaté,[1,2] and Paul Manneville[2,1]
[1]*CEA–Service de Physique de l'Etat Condensé, Centre d'Etudes de Saclay, 91191 Gif-sur-Yvette, France*
[2]*LadHyX–Laboratoire d'Hydrodynamique, Ecole Polytechnique, 91128 Palaiseau, France*
(Received 28 October 1996)

Critical exponents of nonequilibrium, Ising-like phase transitions in two-dimensional lattices of locally coupled chaotic maps are estimated numerically using equilibrium finite-size scaling theory. Numerical data supports the existence of a new universality class, which groups together phase transitions of *synchronously updated* models with Ising symmetry, irrespective of the specific microscopic evolution rule, and of the presence of stochastic noise. However, nonequilibrium, Ising-like phase transitions of asynchronously updated models belong to the Ising universality class. The new universality class differs from the equilibrium Ising universality class by the value of the correlation length exponent, $\nu = 0.89 \pm 0.02$, while exponent ratios β/ν and γ/ν as well as Binder's cumulant U^* assume their usual value. [S1063-651X(97)15703-8]

PACS number(s): 05.45.+b, 05.70.Jk, 64.60.Cn, 47.27.Cn

I. INTRODUCTION

The emergence of long-range order, or collective behavior, in extended dynamical systems with short-range interaction and local chaotic dynamics has attracted considerable attention recently [1–8]. In particular, diffusivelike interaction of identical, chaotic, dissipative dynamical units often gives way to spatiotemporally disordered regimes where chaos becomes *extensive*, that is where quantifiers of chaotic activity—say the Lyapunov dimension or the Kolmogorov-Sinaï entropy—scale with system size [9,10,4]. Intensive quantities, such as entropy densities, are then expected to remain well behaved in the ''thermodynamic'' limit of infinite system size, where simpler effective descriptions of high-dimensional spatiotemporal chaos may become possible. Short of a guiding principle from which invariant measures, order parameters, and other relevant statistical quantifiers can be derived rigorously, the current understanding of the long-wavelength, low-frequency properties of extensively chaotic phases relies heavily on notions borrowed from the better established field of equilibrium statistical mechanics, and adapted to the phenomenology of spatiotemporal chaos [10–14].

Transitions between distinct extensively chaotic regimes are liable to occur when some control parameter is varied, and have been observed in both laboratory and numerical experiments. An interesting example is the transition between two disordered regimes observed in large aspect-ratio Rayleigh-Bénard cells, between a phase dominated by the chaotic interaction of straight convection rolls, and a phase where spiral defects control the large-scale properties of the flow [7]. A natural order parameter is the average curvature of rolls, which may be used to characterize the transition at an aspect ratio fixed by the experimental setup. Another example is given by electrohydrodynamic convection in nematic liquid crystals, known to possess at least two distinct spatiotemporally chaotic regimes. For large enough aspect ratios, an isotropic and an anisotropic phase are separated by a continuous transition [8]. An important, and much studied model of spatiotemporal chaos is the complex Ginzburg-Landau equation, a nonlinear partial differential equation describing the slow modulations of an oscillatory mode close to a supercritical Hopf bifurcation [15]. Large-scale numerical simulations support the existence of two turbulent regimes, defined respectively by the absence and presence of zeros of the amplitude of the complex field, and usually referred to as phase and amplitude turbulence. Due to numerical limitations, the status of this transition—smooth or sharp—as well as the very question of its persistence in the infinite-size limit remain controversial [6].

For lack of adequate theoretical insight, transitions between extensively chaotic phases must be treated in a phenomenological manner, often drawing on intuition based on equilibrium statistical mechanics. While extensively chaotic regimes occur in a wide range of extended dynamical systems, from nonlinear partial differential equations [9] to coupled nonlinear oscillators [16], we concentrate here on coupled map lattices (CML's), or lattices of coupled, iterated maps [17]. CML's provide a convenient testbed for simulating extended systems with local chaos, since their microscopic dynamics can be adjusted at will. An additional motivation is numerical convenience: due to current numerical constraints, CML's are one of the few extensively chaotic systems for which finite-size effects close to transitions can be evaluated accurately enough to yield controlled, reliable extrapolations to the thermodynamic limit.

Lattices of diffusively coupled logistic maps are known to display intriguing, dynamically nontrivial collective behavior, such as periodic and quasiperiodic time evolution of collective variables [1]. Their rich phase diagram includes many collective bifurcations, whose properties are similar to those of phase transitions [18]. Even though time-dependent collective behavior is often seen as a generic property of CML's, the scope of this study will be limited to spontaneously broken parity-reversal invariance, and exclude cases of broken time-translation invariance similar to those reported in [1,18]. Following the recent work of Miller and Huse [3], we choose as a reference the equilibrium two-dimensional

*Present address: Department of Physics, Kyoto University, Kyoto 606, Japan.

Ising model, and consider only CML's whose time-asymptotic statistical properties remain stationary. In this perspective, we present data obtained from numerical simulations of several closely related, CML-like models which exhibit continuous phase transitions akin to the Ising ferromagnetic critical point. We successively address the related, yet separate questions of scaling and universality, with an emphasis on accurate measures of the static critical exponents β, γ, and ν, obtained from equilibrium finite-size scaling laws. Our main result is that Ising-like transitions of CML's respect equilibrium scaling laws, but form a new universality class, associated with a new ''relevant'' parameter [5]: synchronous update, a defining feature of extended dynamical systems. Provided that all lattice sites are updated synchronously, estimates of the correlation-length exponent ν consistently and significantly differ from the Ising exponent $\nu_{\mathrm{Ising}}=1$. We find $\nu_{\mathrm{synchronous}}=0.89\pm0.02$, while the exponent ratios β/ν and γ/ν assume their traditional values of $\frac{1}{8}$ and $\frac{7}{4}$, respectively.

This paper is organized as follows: in Sec. II, the continuous transition of a CML originally introduced in [3] is examined in detail. Following a summary of previous theoretical and numerical work (Sec. II A), we first review the scaling properties of this transition for large system sizes (Sec. II B), before assessing the relevance of equilibrium finite-size scaling laws (Sec. II C). We next demonstrate that the presence of strong corrections to finite-size scaling forbids an estimate of critical exponents accurate enough to decide whether or not this transition belongs to the equilibrium Ising universality class (Sec. II D). The question of universality in continuous transitions of CML's is addressed in Sec. III. The Ising-like transition of a CML with short-range, locally anisotropic coupling rule is introduced in Sec. III A. Thanks to weak corrections to finite-size scaling, we can demonstrate that this transition does not belong to the Ising universality class. Since CML's with different chaotic local maps exhibit the same scaling properties, we conjecture that estimates of critical exponents presented in Sec. II D for Miller and Huse's model are in fact equal to their asymptotic, infinite-size values, and conclude that these transitions form a new universality class. Next, we present evidence according to which synchronous update is the associated ''relevant'' parameter. While the presence of stochastic noise for synchronous update rules (Sec. III B) leads to critical properties identical to those observed in the models of Secs. II and III A, asynchronously updated models turn out to belong to the Ising universality class (Sec. III C). The implications of these results are finally discussed in terms of the notion of weak universality, which may be relevant to far-from-equilibrium models lacking a well-defined temperature (Sec. IV).

II. CONTINUOUS TRANSITION OF A CML: SCALING PROPERTIES

A. General considerations

At equilibrium, phase transitions are usually defined as points in parameter space where a system's partition function becomes nonanalytic in the infinite-size, thermodynamic limit. Transitions are called first or second order according to the singularity order of thermodynamic functions. In particular, second-order transitions are characterized by singular second-order, but smooth first-order derivatives of the free energy: the susceptibility, specific heat, and correlation length all diverge at the transition. On the other hand, the order parameter vanishes in the disordered phase, varies *continuously* in the vicinity of the transition, and acquires nonzero values indicative of a spontaneously broken symmetry in the ordered phase.

The notion of phase transition tends to be used in a somewhat looser manner in far-from-equilibrium, deterministic, many-body systems, for lack of a theoretical framework equivalent to equilibrium statistical mechanics. Apart from a few particular cases [19], determining the invariant measure of coupled dynamical systems remains an impossible task. The partition function and other thermodynamic functions, such as the specific heat, are usually not known. Appropriate order parameters are thus defined on a case-by-case, mostly empirical manner. Low-dimensional dynamical systems without external noise may exhibit symmetry and ergodicity breaking [20]: one may thus question whether symmetry breaking in the thermodynamic limit adequately signals the occurrence of phase transitions in extended dynamical systems [21].

Spatial and temporal correlation functions of local variables can be systematically defined for extended dynamical systems. In fact, they may even form the basis of approximation methods aimed at predicting the emergence of long-range order [22]. The combination of local chaos and diffusive coupling makes most extensively chaotic systems spatially mixing. As a result, equal-time, two-point spatial correlation functions fall off exponentially at generic points in parameter space, allowing for the unambiguous definition of a correlation length. Of course, finite-size systems necessarily possess a finite correlation length. For these reasons, we choose to define the *continuous transition* of an extensively chaotic, extended dynamical system as a point in parameter space where the correlation length associated with local variables diverges in the thermodynamic limit. Further use of the expression ''second-order transition'' will be restricted to equilibrium transitions with nonanalytic thermodynamic functions. Thanks to finite-size scaling methods, we shall later give ample evidence that continuous transitions, as defined above, do occur in CML's.

At equilibrium, the divergence of coherence time and length scales observed at the transition point is responsible for one of the most spectacular properties of second-order phase transitions: universality. The occurrence of fluctuations on all length scales translates quantitatively into scaling laws, which govern the behavior of macroscopic quantities close to the transition. Second-order transitions can then be classified according to the values of the corresponding exponents. Thanks to a diverging correlation length, the numerical value of these critical exponents is insensitive to many details of the underlying physics, as expressed by a microscopic Hamiltonian function. Universality classes, or sets of transitions possessing the same critical exponents, gather physical phenomena of seemingly different nature, provided that a small number of macroscopic constraints are respected. Static exponents of second-order transitions in equilibrium, locally interacting systems without disorder depend only on the type of symmetry broken by the ordered phase

and on the space dimension d [23].

How microscopic details become irrelevant close to the transition point is best understood within the framework of the renormalization group [23]. A coarse-grained Ginzburg-Landau functional is usually postulated to describe the large-scale behavior close to criticality. This functional depends only on the space dimensionality and on symmetries of the system. Thanks to the associated Gibbs measure, contributions arising from small length scales can be integrated out iteratively. Critical exponents are obtained as eigenvalues of the linearized iteration operator close to a (stable) fixed point of the renormalization flow. In many cases, their numerical values can only be calculated perturbatively close to the upper critical dimension d_c, above which fluctuations become irrelevant. A remarkable level of agreement between theory, experiments, and numerical simulations validates the many assumptions involved in this procedure, ranging from the validity of *ad hoc* coarse-grained descriptions to the convergence properties of perturbative expansions.

Some degree of universality is naturally expected to hold for nonequilibrium transitions with a diverging correlation length [24]. A coarse-grained description is then provided by a Langevin equation, i.e., a stochastic partial differential equation for the slow modes ϕ_k of the system, of the following form:

$$\partial_t \phi_k(\vec{x},t) = \mathcal{F}[\phi_k, \vec{\nabla}\phi_k] + \eta(\vec{x},t), \tag{1}$$

where fast, microscopic degrees of freedom are modeled by a Gaussian, δ-correlated white noise $\eta(\vec{x},t)$, and the functional $\mathcal{F}$ describes the (nonlinear) interaction between the n modes $\{\phi_k, k=1,\ldots,n\}$, taking into account all operators compatible with the underlying symmetries. Provided that an equation such as (1) accurately describes the slow modes of the system, the standard prescriptions of the dynamic renormalization group [23–25] lead to sufficient conditions under which a nonequilibrium transition is expected to belong to the universality class of the Ising model, for both static and dynamic critical exponents [26,27]. Irreversible, nonequilibrium contributions become irrelevant close to the fixed point of the renormalization flow provided that the transition is well described by a single, nonconserved, scalar order parameter, and that the underlying model involves only short-range interactions. For conciseness, such transitions will be referred to as *Ising-like transitions* in the following. Note that a microscopic, up-down symmetry is in principle *not* required [27].

In fact, much evidence has been gathered, according to which Langevin equations similar to Eq. (1) faithfully describe the large-scale properties of extensively-chaotic *phases* of extended dynamical systems. Mesoscopic Langevin equations have been successfully applied to systems as diverse as CML's with conserved quantities [11], cellular automata with quasiperiodic time evolution of collective variables [28], or the Kuramoto-Sivashinsky equation, whose large-scale properties are well described by the Kardar-Parisi-Zhang stochastic growth equation [29].

Far less is known about the validity of Langevin descriptions and renormalization group approximations in the vicinity of continuous transitions of extended dynamical systems. A recent study addressing these questions is due to Miller and Huse [3], who introduced a coupled map lattice specifically designed to exhibit an Ising-like continuous transition between two extensively chaotic phases. Their results are twofold: first, the large-scale properties of the (ferromagnetically) ordered phase are well described by the same Langevin equations as used at equilibrium to characterize the slow evolution of antiphase droplets of the Ising model. Second, the static and dynamic critical exponents they measure at the transition are ''consistent with'' the Ising universality class. The first point provides additional evidence that slow modes of extensively chaotic phases usually decouple from their microscopic, chaotic background, which may then be correctly approximated by stochastic noise. In fact, the diffusive relaxation of antiphase droplets they observe can probably be traced back to the diffusive nature of interactions built in the microscopic evolution rule of this CML. On the other hand, we believe that their second conclusion should be taken only *literally*, without hastily proceeding to infer that this critical point *does* belong to the Ising universality class. As we shall show below, answering this question on the basis of data obtained from numerical simulations of this *sole* model would require prohibitively large computing power, due to the occurence of unusually strong corrections to finite-size scaling laws.

B. Continuous phase transition

Coupled map lattices were introduced as generic, numerically economical models of spatio-temporally chaotic reaction-diffusion systems [17]. A CML is well-defined once three ingredients are given: a lattice geometry; a microscopic evolution rule, expressing interaction between neighboring sites; and a local map which governs the reaction part of the time evolution of local variables. In order to produce a ferromagnetic critical point [3], Miller and Huse considered a two-dimensional CML with nearest-neighbor, diffusive coupling on a square lattice and with an odd, chaotic local map. In this section, we introduce their model, and discuss its statistical properties, as observed for large lattices.

The choice of a two-dimensional geometry is motivated by the absence of compelling arguments and of convincing experimental evidence supporting the existence of genuine phase transitions between chaotic phases in one-dimensional extended dynamical systems. To our knowledge, time-dependent collective behavior has never been reported in one-dimensional CML's [1]. Our simulations of the ''phase transition'' of a one-dimensional model reported in [30] does not show any evidence either of critical properties, or of a diverging correlation length. For the complex Ginzburg-Landau equation, the exact status of the transition from defect turbulence to phase turbulence in the infinite-size limit (smooth crossover or true phase transition?) remains unresolved [6]. For all practical purposes, the Mermin-Wagner theorem, stating the impossibility of long-range order in one-dimensional equilibrium systems with short-range interactions, seems to hold true for extensively-chaotic dynamical systems.

Following Miller and Huse, here we consider the simple case of a square, two-dimensional lattice. Nearest-neighbor coupling is chosen in conformity with the equilibrium Ising model. Continuous local variables $x_{i,j}^t$ are assigned to nodes

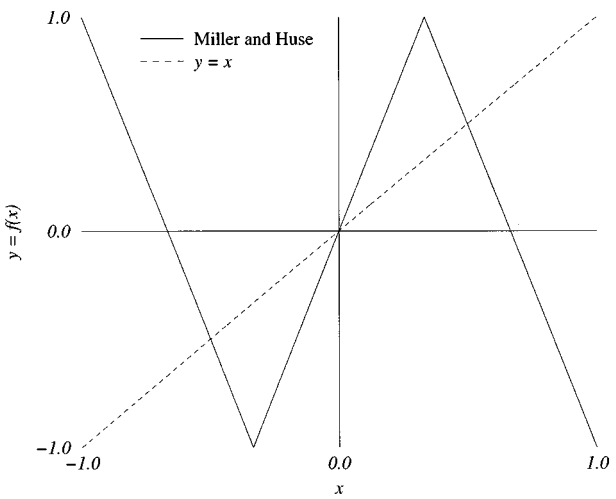

FIG. 1. A graph of the piecewise linear local map of Miller and Huse's model.

of a lattice of linear size L, where indices i and j denote discrete Cartesian coordinates, and t indices discrete time. At each time step t, all sites are updated *synchronously* according to the following evolution rule:

$$x_{i,j}^{t+1}=(1-4g)f(x_{i,j}^{t})+g\big(f(x_{i-1,j}^{t})+f(x_{i,j-1}^{t})+f(x_{i+1,j}^{t}) +f(x_{i,j+1}^{t})\big), \tag{2}$$

where the coupling constant g, a real parameter, takes its values in the real interval $[0,\frac{1}{4}]$ so as to insure the invariance of the CML's phase space under rule (2).

When the local phase space is a parity-invariant interval, spin variables $\sigma_{i,j}^{t}$ can be naturally defined as

$$\sigma_{i,j}^{t}=\mathrm{sgn}(x_{i,j}^{t})\in\{-1,1\}. \tag{3}$$

Combining this remark with the additional requirement of local chaos, Miller and Huse were led to the choice of the odd, piecewise linear, everywhere expanding map defined on the bounded interval $[-1,1]$ by (Fig. 1)

$$f(x)=\begin{cases} -3x-2 & \text{if } -1\leqslant x\leqslant -\dfrac{1}{3} \\ 3x & \text{if } -\dfrac{1}{3}\leqslant x\leqslant \dfrac{1}{3} \\ -3x+2 & \text{if } \dfrac{1}{3}\leqslant x\leqslant 1. \end{cases} \tag{4}$$

This map is chaotic, its positive Lyapunov exponent is equal to ln3, and its invariant measure is uniform on $[-1,1]$.

For numerical convenience, the evolution rule (2) is supplemented with periodic boundary conditions. Starting from random initial conditions uniformly distributed in $[-1,1]$, a unique attracting steady state is reached after a generally short relaxation time. Depending on the coupling strength g, two qualitatively distinct regimes are observed (Fig. 2): for values smaller than a critical coupling strength denoted g_c, the CML is ''paramagnetic,'' since positive (up) and negative (down) spins are equiprobable. Above g_c, an

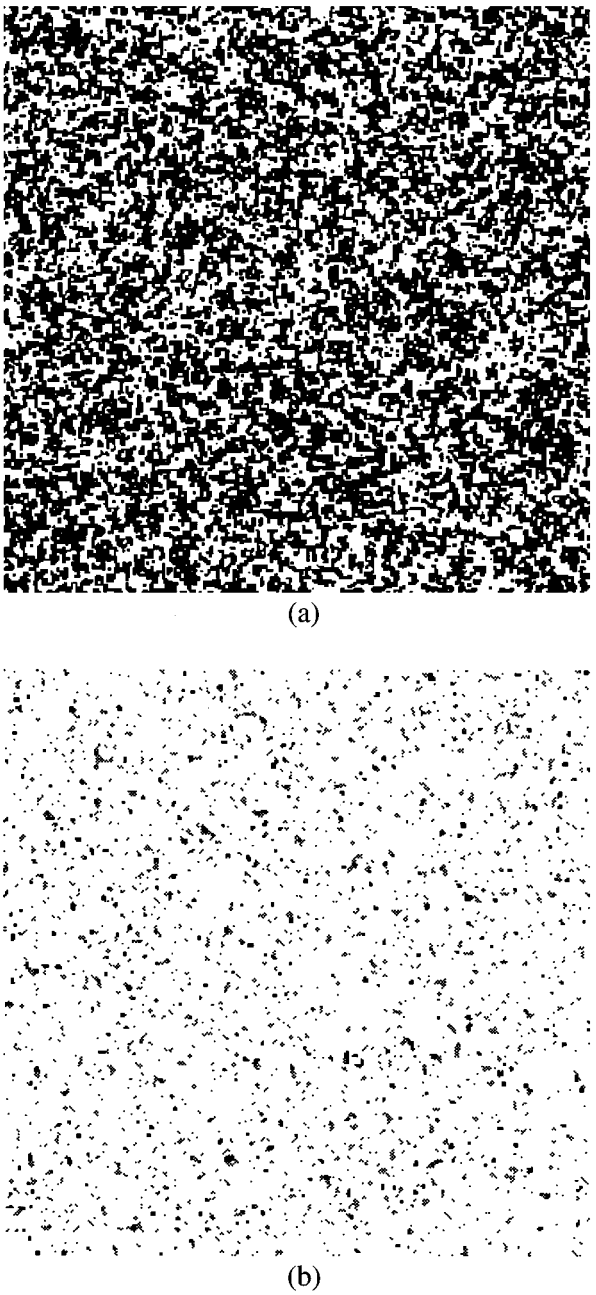

FIG. 2. Typical snapshots of Miller and Huse's model, in time-asymptotic regimes observed far from the transition point $g_c\sim 0.205$ for a linear size $L=400$. Up- and down-spins are represented by black and white pixels, respectively. (a) Disordered, ''paramagnetic'' phase, $g=0.18$. (b) Ordered, ''ferromagnetic'' phase, $g=0.23$.

increased rigidity leads to the (dynamical) selection of a preferred sign: the CML exhibits ferromagnetic long-range order. Both phases are extensively chaotic, as can be checked, for instance, from numerical estimates of the Kolmogorov-Sinaï entropy obtained for different lattice sizes. They are examples of ''fully developed spatiotemporal chaos,'' the strong-coupling regime of many diffusively coupled CML's, as was first observed by Kaneko in coupled logistic maps [31].

Ergodicity being assumed, the ensemble average $\langle A\rangle$ of any observable A of the CML is equated with its temporal

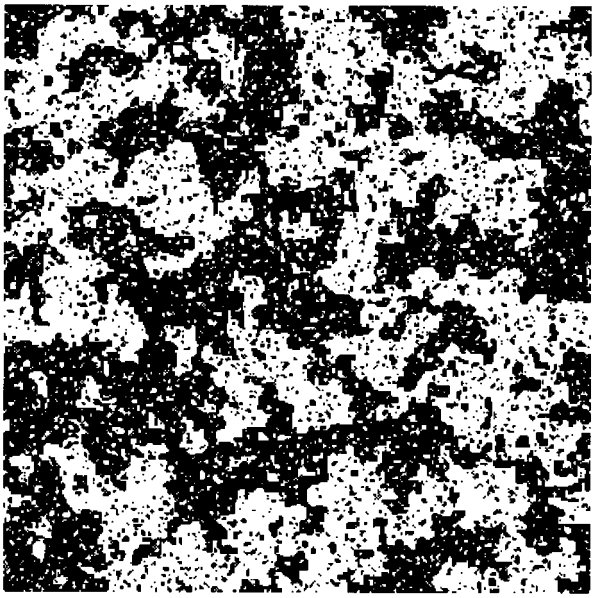

FIG. 3. A typical snapshot of Miller and Huse's model close to its transition point, obtained in the time-asymptotic regime for $L=400$ and $g=0.205\simeq g_c(L=400)$. Up- and down-spins are represented by black and white pixels, respectively.

average, and in practice computed along a trajectory as

$$\langle A\rangle=\frac{1}{t_m+1}\sum_{t=t_0}^{t=t_0+t_m}A^t, \tag{5}$$

where t_0 and t_m, respectively, denote the duration of discarded transients, and the (sufficiently long) integration time. Note that relaxation times toward the attractor may become long, in the ferromagnetic phase, due to the diffusivelike decay of large antiphase droplets which may arise from exceptional initial conditions. In the following, care has been taken to insure that the observed statistical properties do indeed correspond to the time-asymptotic, stationary regime.

Spatial patterns are homogeneous and isotropic on length scales large compared to the lattice step. Macroscopic quantities such as the averaged activity $\langle x\rangle$ may thus be obtained either from the time average of a local variable $x^t_{i_0,j_0}$, for any fixed lattice site of coordinates (i_0,j_0), or from that of the space average of $x^t_{i,j}$ computed over the lattice. For all (normed) vector $\vec{v}$ of the plane, a one-dimensional, equal-time, two-point spatial correlation function $C_{\vec{v}}(r)$ can be defined along direction $\vec{v}$. The spatial extension of clusters of aligned spins in the disordered phase is of the order of a few lattice steps far from the transition point g_c [see Fig. 2(a)]. The exponential decay of correlation functions $C_{\vec{v}}(r)$ leads to the natural definition of correlation lengths denoted $\xi_{\vec{v}}$. In fact, neither the functional form of $C_{\vec{v}}(r)$ nor the numerical value of $\xi_{\vec{v}}$ depend on the choice of the direction $\vec{v}$: this isotropic system is well described by a unique correlation length ξ.

Snapshots taken close to the transition show the formation of clusters of spins on all length scales comprised between the CML's natural cut-off scales, i.e., between 1 and L lattice steps (cf. Fig. 3). The accompanying algebraic decay of the correlation function (not shown) suggests that the correlation length may diverge at that point in the thermodynamic limit, signaling the occurrence of a continuous phase transition. We now proceed to the definition of the corresponding order parameter.

For a finite-size lattice, the instantaneous magnetization is defined as the spatial average of spin values:

$$m^t_L=\frac{1}{L^2}\sum_{i,j}\sigma^t_{i,j}. \tag{6}$$

Note that the local spins $\sigma^t_{i,j}$ are intermediate variables which do not take a direct part in the dynamics. Because of finite-size effects, sign reversals of m^t_L occur in the ordered phase, on a time scale long compared to that of its fluctuations. It is therefore customary to define the finite-size order parameter M_L as [32]

$$M_L=\langle|m^t_L|\rangle=\frac{1}{t_m+1}\sum_{t=t_0}^{t=t_0+t_m}|m^t_L|, \tag{7}$$

whereby the ordered phase exhibits non-zero values of the finite-size magnetization M_L. Note that the average interval of time between two sign reversals of the instantaneous magnetization diverges with system size [21], an indication that ergodicity breaking and symmetry breaking occur only in the thermodynamic limit.

The susceptibility of equilibrium Ising systems is traditionally defined as the response of the order parameter to an external perturbation. For lack of a standard, unambiguous way to couple the CML to an external field [11], we choose to define the finite-size susceptibility χ_L as follows:

$$\chi_L=L^2\langle(|m^t_L|-M_L)^2\rangle, \tag{8}$$

where the average $\langle\rangle$ is computed as in Eq. (5).

Close to the transition, we checked that both magnetization and susceptibility depend algebraically on the distance to criticality (see Fig. 4 for our raw data). In the infinite-size limit, the following power laws are expected to apply:

$$M\sim(g-g_c)^\beta \quad \text{for } g\geqslant g_c,$$
$$\chi\sim|g-g_c|^{-\gamma},$$
$$\xi\sim|g-g_c|^{-\nu}, \tag{9}$$

where β, γ, and ν are the usual static critical exponents [23]. As a first step, we estimate the effective exponents β_{1024} and γ_{1024}, defined for a finite size $L=1024$ as

$$M_{1024}\sim(g-g_c(1024))^{\beta_{1024}} \quad \text{for } g\geqslant g_c(1024),$$
$$\chi_{1024}\sim|g-g_c(1024)|^{-\gamma_{1024}}, \tag{10}$$

where $g_c(1024)$ is the effective transition point. In order to avoid notoriously inaccurate nonlinear fits for several unknown variables, our measurement protocol is as follows. For a fixed value of $g_c(1024)$, we fit the log-log plot of, say, magnetization vs distance to criticality by a straight line, and thus obtain a first, g-dependent estimate of β_{1024}. Our final

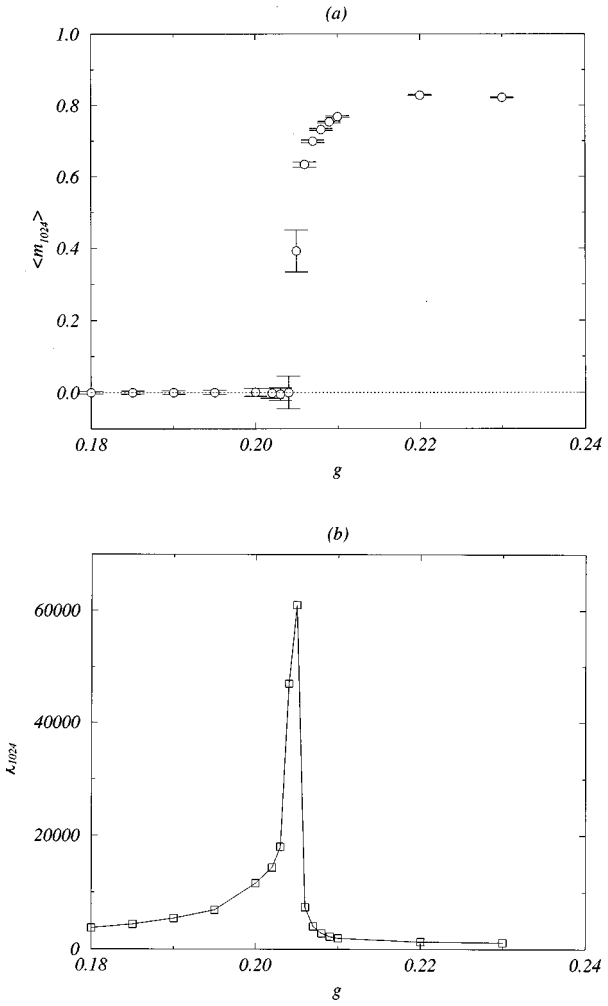

FIG. 4. Macroscopic quantifiers of Miller and Huse's model. Plots of (a) the magnetization $\langle m_{1024}\rangle$ and (b) the susceptibility χ_{1024} are presented as a function of the coupling constant g for a large size $L=1024$. Time averages are performed over a sampling time $t_m \sim O(10^5)$. In this case, the magnetization can be computed without an absolute value, since t_m is much smaller than the sign-reversal time-scale.

stimate of $g_c(1024)$ and β_{1024} corresponds to the optimal fit within a reasonable interval of values of $g_c(1024)$, defined as the locus on the g axis of a local maximum of the quality coefficient of fits. The same procedure is applied to both magnetization and susceptibility data, and yields mutually consistent values of the critical point. Our estimates are

$$g_c(L=1024)\simeq 0.20515,$$

$$\beta_{1024}\simeq 0.09,$$

$$\gamma_{1024}\simeq 1.48. \tag{11}$$

These values are obviously *not* consistent with Ising exponents.

In this section, no attempt is made to provide error bars on values (11), which may arise from a combination of finite size effects, finite equilibration time effects and systematic deviations due to the choice of the measurement procedure. In [3], Miller and Huse only claimed ''consistency'' with Ising values, yet did not attempt to measure the values of critical exponents directly, nor to investigate the strength and influence of finite-size effects. Since their results were obtained for significantly smaller lattices, our estimates [Eq. (11)] suggest that finite-size effects are indeed strong in this system, and can by no means be neglected. This essential point will be tackled in the following section, whose main purpose is to check the validity of values (11), thanks to a finite-size scaling analysis of statistical properties close to the critical point. This in turn gives way to controlled extrapolations of finite-size quantities in the infinite-size limit, and to reliable error bars on estimates of g_c, β, γ, and ν.

C. Finite-size scaling

Even though finite-size systems at equilibrium do not undergo true phase transitions, their behavior close to the (infinite-size) transition point provides useful quantitative information on properties valid in the thermodynamic limit. At equilibrium, the bulk free energy F of an isotropic, d-dimensional magnetic system of finite size L, subject to an external field B at temperature T, can be written close to the transition point under the following scaling form, up to correction terms which we choose to ignore for the moment:

$$F(T,B,L)=L^{-d}\hat{F}(|T-T_c^{\infty}|L^{1/\nu},BL^{(\beta+\gamma)/\nu}), \tag{12}$$

where $\hat{F}$ is the rescaled free-energy function and T_c^{∞} is the infinite-size critical temperature (see [32] for recent reviews on finite-size scaling and [33] for seminal papers). One can easily show that Eq. (12) leads, at the critical temperature T_c^{∞} and under zero external field, to finite-size scaling laws for the magnetization and susceptibility:

$$M_L(T_c^{\infty})\sim L^{-\beta/\nu},$$

$$\chi_L(T_c^{\infty})\sim L^{\gamma/\nu}. \tag{13}$$

The exponents used in Eqs. (12) and (13) are identical to the standard, infinite-size quantities β, γ, and ν. These relations thus provide a convenient way to estimate their numerical values from finite-size simulations.

From an experimental viewpoint, a finite-size system correctly approximates the infinite-size limit when its size is much larger than its correlation-length: $L \gg \xi_L$. Of course, this cannot remain true infinitely close to T_c^{∞}, where the correlation length diverges. Finite-size scaling is thus expected to apply as soon as $L \lesssim \xi_L$, i.e., sufficiently close to the transition point. Even though we are unable to define explicitly an effective, coarse-grained free energy for Miller and Huse's CML in the spirit of Eq. (12), we expect the same quantitative behavior to apply to its nonequilibrium continuous transition for the following reasons.

(i) The phase transition of this model appears to be well defined in the thermodynamic limit only, as shown by our investigations (see Sec. II B), as well as by numerical measures of the average sign-reversal time in the ordered phase [21].

(ii) Only *one* length scale diverges at the transition: the correlation length ξ_L. The CML is isotropic at large enough

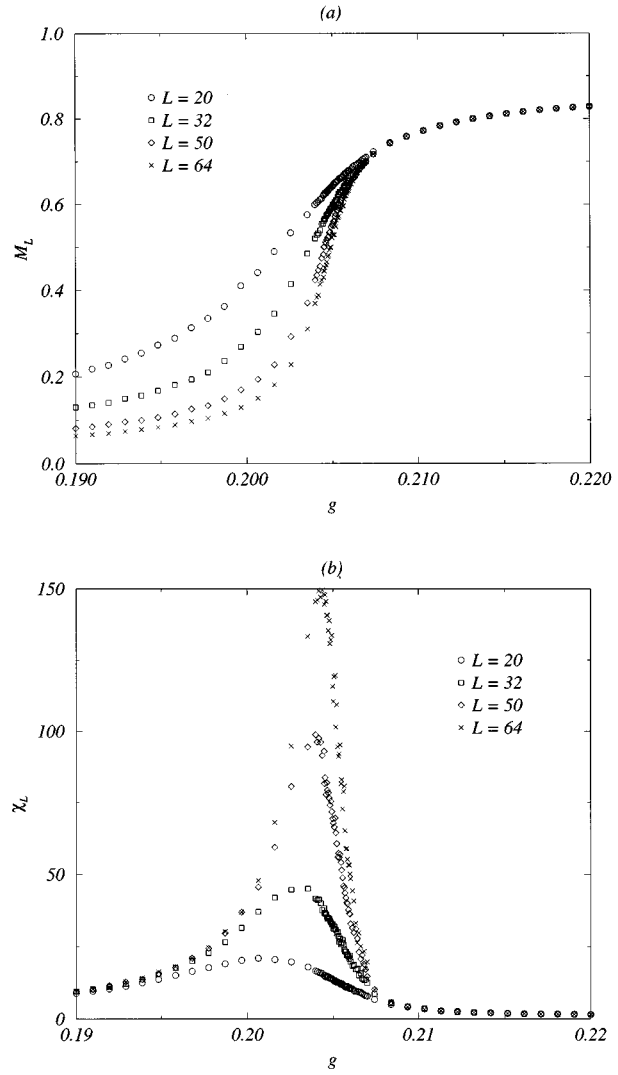

FIG. 5. Size dependence of the macroscopic quantifiers of Miller and Huse's model. Plots of (a) the magnetization M_L and (b) the susceptibility χ_L are presented as a function of the coupling constant g, for four different system sizes $20 \leqslant L \leqslant 64$. A time average is performed over $t_m \sim O(10^7)$, a time scale much larger than the average time between two sign reversals of the instantaneous magnetization. The transition is rounded and shifted due to finite-size effects.

length scales. Length scales related to dynamic quantifiers, such as the Lyapunov dimension, vary smoothly close to the transition [4]. Even though a proper finite-size study of this result remains to be conducted, this suggests that the onset of long-range order is decoupled from the CML's microscopic dynamics.

We now provide qualitative and quantitative evidence supporting the relevance of Eq. (12) to Miller and Huse's CML. In Fig. 5, we show plots of the CML's order parameter and susceptibility vs coupling constant for system sizes ranging from $L=20$ to 64. Experimental conditions are unchanged, with integration times $t_m \sim O(10^7)$. As expected, the divergence of the susceptibility is rounded and shifted over some parameter region, while the magnetization decreases smoothly to a small constant value in the disordered phase (see Fig. 4 for comparison).

Let g_c^∞ denote the infinite-size transition coupling constant. Scaling laws similar to Eqs. (13) are expected to hold in a neighborhood of this point, e.g.,

$$M_L(g) \sim L^{-\hat{\beta}(g)}, \quad g \in \mathcal{V}(g_c^\infty), \tag{14}$$

where $\hat{\beta}(g)$ is a smooth function of g. Therefore, reliable values for the exponent ratios $\beta/\nu$and γ/ν can only be obtained once g_c^∞ is known with sufficient accuracy. From Fig. 5(b), we see that an effective critical coupling constant $g_c(L)$ can be defined for a given finite size L as the abscissa of the global maximum of χ_L. Our data is consistent with the following scaling law [33]:

$$g_c(L) - g_c^\infty \propto L^{-1/\nu}, \tag{15}$$

which can be fitted simultaneously for g_c^∞ and ν. However, we prefer to evaluate g_c^∞ independently of the exponent ν. A useful quantity is Binder's cumulant $U_L(g)$ [34], defined as

$$U_L(g) = -3 + M_L^{(4)}(g)/(M_L^{(2)}(g))^2, \tag{16}$$

where $M_L^{(k)}$ denotes the kth-order moment of the magnetization $M_L^{(k)} = \langle (m_L^t)^k \rangle$. According to the same analogy with equilibrium second-order transitions [Eq. (12)], we are led to write the scaled form of Binder's cumulant as

$$U_L(g) = \hat{U}((g - g_c^\infty) L^{1/\nu}). \tag{17}$$

Remarkably, size-dependent prefactors cancel on the right-hand side of Eq. (17) [34]. As a result, $U_L(g)$ becomes independent of L at criticality,

$$U_L(g_c^\infty) = U^*, \forall L. \tag{18}$$

At equilibrium, the quantity U^* is a universal ratio of amplitudes. Its numerical value is estimated to be $-U^* \sim 1.830$–1.835 for the Ising universality class (see [35] for further references).

In practice, our estimate g_c^∞ is determined by plotting graphs of $U_L(g)$ vs g for system sizes ranging from $L=32$ to 128 (Fig. 6). The simulation times—typically 10^3 times the coherence time—are long enough in order to achieve satisfactory statistical accuracy. Error bars then correspond to the extension of the intersection region. Our estimates are

$$g_c^\infty = 0.205\ 34(2),$$
$$-U^*(g_c^\infty) = 1.832(4), \tag{19}$$

where numbers between brackets correspond to the uncertainty on the last digit(s) of the measured quantity: $g_c^\infty = 0.205\ 34 \pm 0.000\ 02$, $-U^*(g_c^\infty) = 1.832 \pm 0.004$. Even for the largest sizes considered $[(L_1, L_2) = (64, 128)]$, a slow drift toward larger values of g is observed when comparing the successive locations of the intersection points of curves $U_{L_1}(g)$ and $U_{L_2}(g)$. Accordingly, a systematic uncertainty on the position of the infinite-size critical point cannot be excluded. Note, however, that the value of U^* given in Eq. (19) is in remarkable agreement with that expected for the Ising universality class.

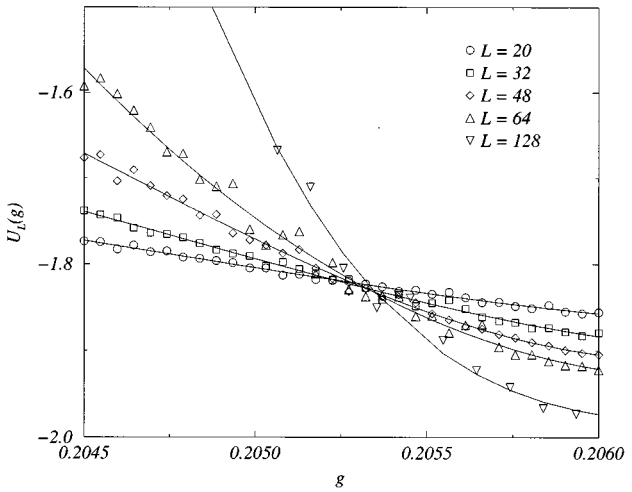

FIG. 6. Illustration of the relevance of Binder's method when estimating the critical coupling constant of the continuous transition of Miller and Huse's model. Plots of Binder's cumulant with respect to g are presented for system sizes $20 \leqslant L \leqslant 128$. Symbols correspond to raw data, plain lines to polynomial fits. Estimates for g_c^∞ and U^* reflect the size of the intersection region of curves obtained for sizes $32 \leqslant L \leqslant 128$.

We now proceed to measure exponent ratios β/ν, γ/ν and $1/\nu$. Figure 7 shows that the expected scaling laws:

$$M_L(g_c^\infty) \sim L^{-\beta/\nu},$$

$$\chi_L(g_c^\infty) \sim L^{\gamma/\nu} \tag{20}$$

are indeed respected when g_c^∞ is equal to its measured value (19). Linear fits in the log-log scale for $20 \leqslant L \leqslant 64$ lead to the estimates

$$\beta/\nu = 0.125(4),$$

$$\gamma/\nu = 1.761(10), \tag{21}$$

in good agreement with the Ising values $(\beta/\nu)_{\text{Ising}} = \frac{1}{8}$ and $(\gamma/\nu)_{\text{Ising}} = \frac{7}{4}$. The main source of error stems from the uncertainty on g_c^∞.

In order to measure ν, we choose to use the scaling laws

$$\partial_g U_L(g_c^\infty) \sim L^{1/\nu},$$

$$\partial_g \ln M_L^{(2)}(g_c^\infty) \sim L^{1/\nu},$$

$$\partial_g \ln M_L(g_c^\infty) \sim L^{1/\nu}, \tag{22}$$

easily derived from Eq. (12) [32]. Even though only the first and second moments of the magnetization will be considered here for computational reasons, logarithmic derivatives of all higher-order moments also scale with L with a dominant exponent equal to $1/\nu$. At equilibrium, numerical differentiation of noisy data can be avoided: derivatives on the left-hand side of Eq. (22) can be expressed as combinations of moments by using the properties of the Boltzmann weight. This is, however, not possible in this case. An alternative method consists in approximating the derivative [e.g., $\partial_g U_L(g_c^\infty)$] by a finite difference taken between two neighboring points g_c^- and g_c^+, $g_c^- < g_c^\infty < g_c^+$. This method turns out to be difficult to control, and is overly sensitive to statistical errors on the values of the original data, in this case $U_L(g_c^+)$ and $U_L(g_c^-)$. We choose instead to first fit the experimental *curve* $U_L(g)$, by a polynomial function $P(g)$, and then approximate the derivative by the polynomial's derivative at the critical point: $\partial_g U_L(g_c^\infty) \simeq P'(g_c^\infty)$. When a sufficient number of data points spread over a large enough interval of g values are considered, the numerical value $P'(g_c^\infty)$ turns out to be independent of the degree of the polynomial P. Figure 8 shows plots, drawn on a log-log scale, of the quantities $\partial_g U_L(g_c^\infty)$, $\partial_g \ln M_L(g_c^\infty)$ and $\partial_g \ln M_L^{(2)}(g_c^\infty)$ thus obtained. Corrections to scaling are clearly present for the smallest sizes. Linear fits on the four rightmost points of each data set in Fig. 8 ($32 \leqslant L \leqslant 64$) lead to the following estimate:

$$\nu = 0.874(17). \tag{23}$$

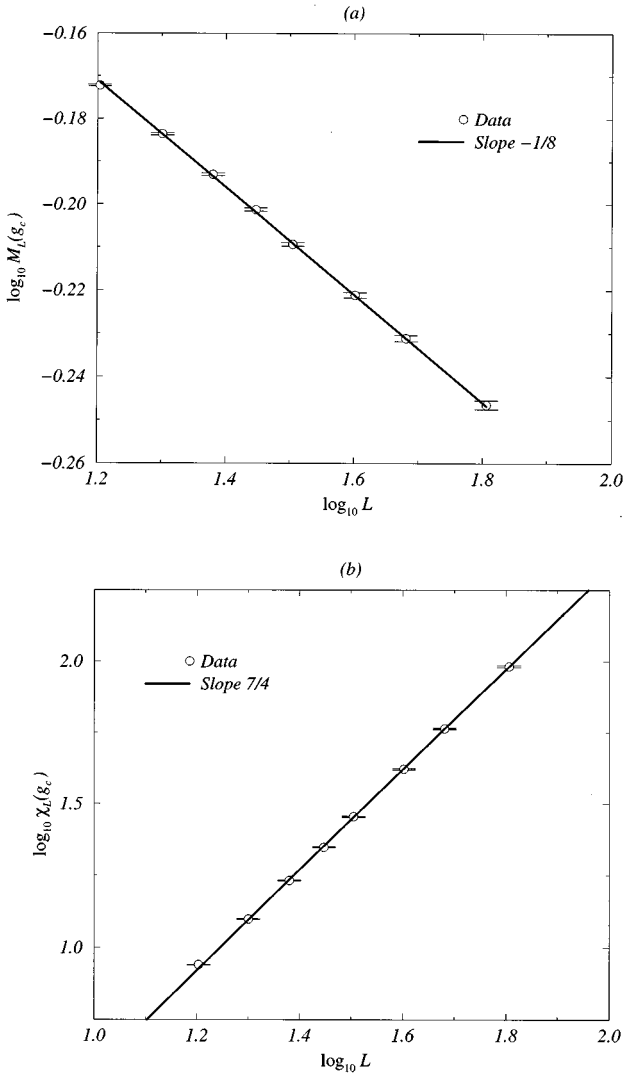

FIG. 7. Measure of the critical ratios β/ν and γ/ν for Miller and Huse's model. Log-log plots of (a) the magnetization $M_L(g_c)$ and (b) the susceptibility $\chi_L(g_c)$ vs system size are presented at criticality [$g_c = g_c^\infty = 0.205\,34(2)$]. The solid lines correspond to Ising exponents, in good agreement with numerical data. Note the weakness of corrections to dominant scaling.

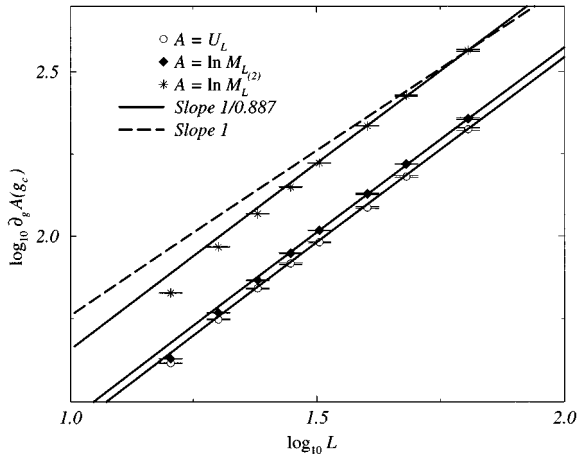

FIG. 8. Direct measure of the correlation-length exponent ν for Miller and Huse's model. Log-log plots of the derivatives of $U_L(g_c)$, $\ln M_L(g_c)$, and $\ln M_L^{(2)}(g_c)$ vs system size are presented at the critical point, $g_c = g_c^\infty = 0.205\,34(2)$, for system sizes in the range $16 \leqslant L \leqslant 64$. Straight lines of slope $1/\nu_{\text{Ising}} = 1$ and 1/0.887 are drawn. Strong corrections to dominant scaling are present. The value of $\nu_{\text{ref}} = 0.887$, our reference, is obtained from the same data by taking into account a single corrective exponent (cf. Sec. II D). Visually, this slope hardly differs from 1/0.874, as obtained from Sec. II C's estimate $\nu = 0.874$, which overlooks possible corrections to scaling.

As before, the main source of uncertainty derives from the error bars affecting the value of g_c^∞. Note that our measurement protocol leads to mutually consistent behavior for the three quantities in Eq. (22), even though one would in principle expect the stability and accuracy of measures to be ordered as

$$\partial_g U_L(g_c^\infty) \lesssim \partial_g \ln M_L^{(2)}(g_c^\infty) \lesssim \partial_g \ln M_L(g_c^\infty), \qquad (24)$$

since statistical accuracy decreases with the order of moments of m_L^t involved.

In this section, we have first of all confirmed—albeit indirectly—the validity of Eq. (12) for the nonequilibrium continuous transition of Miller and Huse's CML. However, our quantitative estimates of critical exponents are in partial disagreement with the conclusions of [3]: while the ratios β/ν and γ/ν agree with Ising values, our—so far naive—estimate of ν is not compatible with the Ising correlation-length exponent $\nu_{\text{Ising}} = 1$. In Sec. II D, we attempt to answer the following question: does this discrepancy reveal actual asymptotic behavior, or is it only due to the presence, for small systems, of corrections to dominant scaling which might obscure the true, infinite-size behavior?

D. Corrections to finite-size scaling

The relevance of corrections to dominant scaling laws is perhaps best shown by graphs of the quantities $\partial_g U_L(g_c^\infty)/L^{1/\nu}$, $\partial_g \ln M_L(g_c^\infty)/L^{1/\nu}$, and $\partial_g \ln M_L^{(2)}(g_c^\infty)/L^{1/\nu}$ vs system size L. When the numerical value $\nu = 0.887$ is used [cf. Eq. (30)], such graphs show clear evidence of convergence towards well-defined limit [Fig. 9(a)]. The same comment is valid for $\nu = 0.874$ [Eq. (23)]. Nonetheless, plots obtained for $\nu = \nu_{\text{Ising}} = 1$ [Fig. 9(b)] have not reached

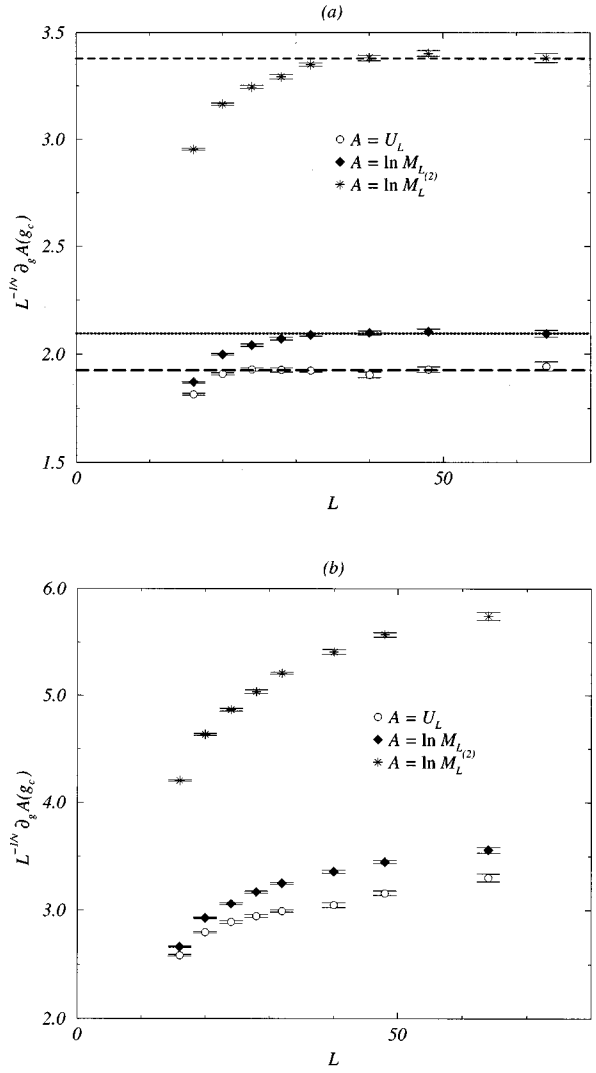

FIG. 9. A convenient display of corrections to dominant scaling affecting the measure of ν for Miller and Huse's model. Lin-lin plots of the quantities $\partial_g U_L(g_c)/L^{1/\nu}$, $\partial_g \ln M_L(g_c)/L^{1/\nu}$, and $\partial_g \ln M_L^{(2)}(g_c)/L^{1/\nu}$ are presented at criticality $[g_c = g_c^\infty = 0.205\,34(2)]$ vs system size L. In graph (a), rapid convergence to a plateau which may faithfully represent infinite-size behavior is reached for our estimate $\nu = 0.887$. Using $\nu = \nu_{\text{Ising}} = 1.0$ instead [graph (b)] leads to possible, but extremely late convergence (see text).

saturation for $L \leqslant 64$. However, a very slow convergence cannot be ruled out for very large system sizes.

In order to assess quantitatively the validity of this observation, we turn once more to results known to hold at equilibrium. According to renormalization group theory, convergence toward asymptotic behavior is generically controlled by irrelevant operators, i.e., operators whose eigenvalues close to the relevant fixed point are negative. For finite-size systems, the scaling form of the free energy becomes, in the simplest case,

$$F(T,B,L) = L^{-d} \hat{F}((T - T_c^\infty) L^{1/\nu}, B L^{(\beta+\gamma)/\nu}, \mathcal{S}_{\text{irr}} L^{-\omega/\nu}), \qquad (25)$$

where only one irrelevant scaling field $\mathcal{S}_{\text{irr}}$ is included, and ω is the associated (positive) corrective exponent. In prac-

tice, deviations from asymptotic scaling laws under zero external field derive both from the presence of irrelevant operators and from the experimental uncertainty on the location on the infinite-size critical point. The large size behavior of thermodynamic quantities is then controlled by a double expansion in powers of $L^{-\omega}$ and of the reduced temperature $(T-T_c^{\infty})L^{1/\nu}$.

Assuming that an equation analogous to Eq. (25) is valid for Miller and Huse's CML, we obtain the following expressions:

$$M_L(g)=L^{-\beta/\nu}(a_0+a_1L^{-\omega}+\cdots+b_1(g-g_c^{\infty})L^{1/\nu}+\cdots),$$

$$\chi_L(g)=L^{\gamma/\nu}(c_0+c_1L^{-\omega}+\cdots+d_1(g-g_c^{\infty})L^{1/\nu}+\cdots),$$

$$\partial_g U_L(g)=L^{1/\nu}(e_0+e_1L^{-\omega}+\cdots+f_1(g-g_c^{\infty})L^{1/\nu}+\cdots),$$

$$\partial_g \ln M_L(g)=L^{1/\nu}(q_0+q_1L^{-\omega}+\cdots+r_1(g-g_c^{\infty})L^{1/\nu}+\cdots),$$

$$\partial_g \ln M_L^{(2)}(g)=L^{1/\nu}(s_0+s_1L^{-\omega}+\cdots+t_1(g-g_c^{\infty})L^{1/\nu}+\cdots), \tag{26}$$

where $a_n, b_n, \ldots, n=0,1,\ldots$ are nonuniversal, real parameters. A simpler ansatz is, however, necessary, since each of these equations already involves a larger number of unknown variables than can be expected to be determined reliably from the available data points. Inspection of both graphs of Fig. 9 reveals qualitative consistency with the presence of one corrective exponent, as in Eq. (26). In addition, the growth of error bars with system size can be interpreted, for data of similar statistical accuracy, as deriving from the presence of a correction term such as $(g-g_c^{\infty})L^{1/\nu}$. Since our main goal is to improve the reliability of estimates of the critical exponent ν, we choose to take into account one *effective* exponent $\omega(g)$, as in the expression

$$\partial_g \ln M_L^{(2)}(g)=L^{1/\nu(g)}(s_0(g)+s_1(g)L^{-\omega(g)}), \tag{27}$$

where $\nu(g)$, $\omega(g)$, $s_0(g)$, and $s_1(g)$ are smooth functions of the coupling constant g. Error bars on, e.g., ν, then correspond to the range covered by values of $\nu(g)$ when g varies within the confidence interval obtained for the critical coupling g_c^{∞}.

We now describe our measurement protocol in the particular case of $\partial_g \ln M_L^{(2)}(g_c^{\infty})$. Generalization to other ''thermodynamic'' quantities on the left-hand side of Eq. (26) is straightforward. Let g_c assume a fixed value in the confidence interval previously obtained for g_c^{∞} [cf. Eq. (19)]. For fixed, reasonable values of (ν,ω), we plot $L^{-1/\nu}\partial_g \ln M_L^{(2)}(g_c)$ with respect to $L^{-\omega}$. A *linear* fit leads to a first estimate of $s_0(g_c,\nu,\omega)$ and $s_1(g_c,\nu,\omega)$, as well as of the corresponding $\chi^2(g_c,\nu,\omega)$ measuring the quality of the fit—not to be confused with the critical susceptiblity $\chi(g_c)$. The critical coupling g_c being fixed, we determine the exponents $(\nu(g_c),\omega(g_c))$ from the best fit, defined as the locus of a local minimum $\chi^2(g_c)=\min\chi^2(g_c,\nu,\omega)$. In practice, a clear minimum of the function $\chi^2(g_c,\nu,\omega)$ is observed, and correponds to fits of good quality [cf. Fig. 10; a projection on the plane $\omega=\omega(g_c)$ is used for clarity in Fig. 10(a)]. The final error bars on ν and ω correspond to the extremal values obtained when applying the same protocol while varying

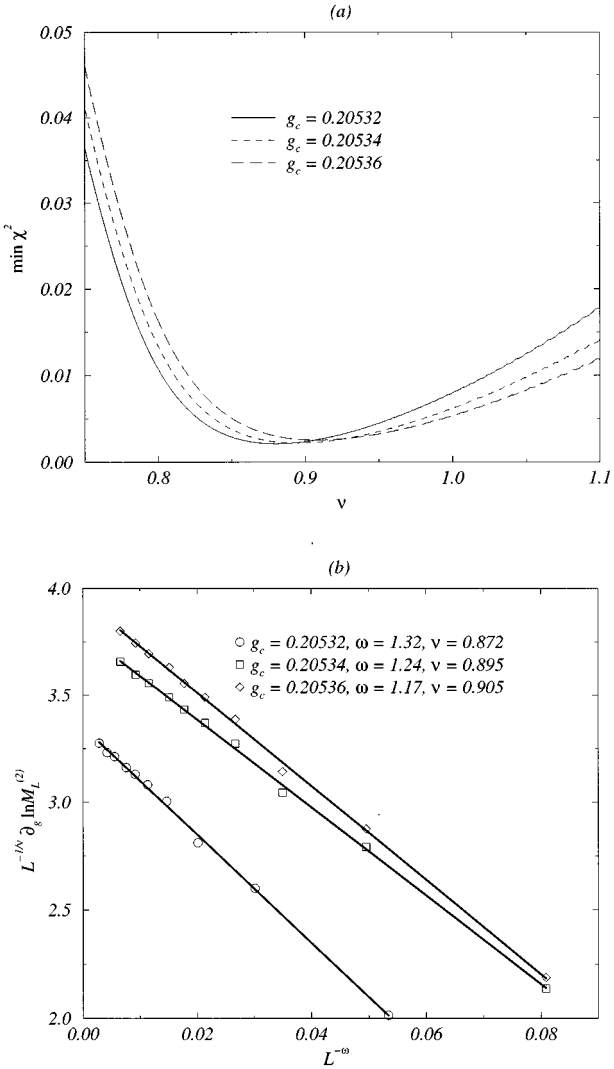

FIG. 10. An estimate of the effective, corrective exponent ω_ν for Miller and Huse's CML. Plots of χ^2 vs ν, obtained for an already optimized value of ω_ν, are shown in graph (a) for three fixed values of the critical coupling constant spanning the confidence interval $g_c=g_c^{\infty}\in[0.205\,32, 0.205\,36]$. Linear fits corresponding to the minima of the three curves are presented in graph (b), where symbols denote our data, obtained in each case for the optimal triplet (g_c,ω,ν).

g_c over the relevant interval. The three quantities $\partial_g U_L(g_c^{\infty})/L^{1/\nu}$, $\partial_g \ln M_L^{(2)}(g_c^{\infty})/L^{1/\nu}$ and $\partial_g \ln M_L(g_c^{\infty})/L^{1/\nu}$ are analyzed along the same lines, yielding mutually consistent results. Our global estimate is

$$\nu=0.887(18), \quad \omega_\nu=1.5\pm0.4. \tag{28}$$

This value of ω is compatible with a rapid relaxation to an asymptotic behavior reached as soon as $L=32$, in agreement with Fig. 9(b).

Applying the same method to exponent ratios β/ν and γ/ν yields the following estimates:

$$\beta/\nu=0.125(4), \quad \omega_M=9(4),$$

$$\gamma/\nu=1.748(10), \quad \omega_\chi=5.7(5). \tag{29}$$

TABLE I. Critical exponents of Ising-like phase transitions of CML's. For each model, we give numerical estimates of the critical point g_c^∞, Binder's cumulant $-U^*$, and the three static critical exponents β, γ, and ν. The ratio $(2\beta+\gamma)/\nu \sim 2.0$ is everywhere in agreement with an hyperscaling relationship. The abbreviations MH4, $C4$, and MH3 correspond respectively to Miller and Huse's model, to the CML with cubic map discussed in Sec. III A 1, and to the locally anisotropic, three-neighbor coupling CML of Sec. III A 2. The three transitions belong to the same (non-Ising) universality class.

	MH4	MH3	$C4$
g_c^∞	0.205 34(2)	0.251 18(4)	0.178 64(4)
$-U^*$	1.832(4)	1.823(3)	1.83(1)
β/ν	0.125(4)	0.131(6)	0.125(7)
γ/ν	1.748(10)	1.74(3)	1.75(4)
$(2\beta+\gamma)/\nu$	2.00(2)	2.01(4)	2.00(5)
β	0.111(5)	0.117(7)	0.114(11)
γ	1.55(4)	1.55(5)	1.60(11)
ν	0.887(18)	0.895(12)	0.91(4)

Taking into account one corrective exponent leads here to improved agreement with Ising values. The large values of ω_M and ω_χ are consistent with a fast relaxation to asymptotic behavior, as observed in Fig. 7. The discrepancies observed in the measured values of ω_ν, ω_M, and ω_χ apparently contradict Eq. (26), where a single exponent ω is present. This is easily accounted for by remembering that ω as measured here is an effective corrective exponent, integrating all possible sources of corrections to scaling. An accurate determination of the (unique) exponent ω would require data of much better statistical quality. Combining Eqs. (28) and (29), we obtain the following final estimates of critical exponents:

$$\beta = 0.111(5),$$

$$\gamma = 1.55(4),$$

$$\nu = 0.887(18), \tag{30}$$

as reported in Table I, where Miller and Huse's CML is referred to as MH4.

Assuming that the exponent ν holds its Ising value, we implement the same protocol, this time varying only g and ω. Within this constraint, the ''best fit'' can no longer correspond to a global minimum of $\chi^2(g_c,\nu,\omega)$ [cf. Fig. 10(a)]. The value thus obtained for ω_{Ising} is smaller than 1:

$$\nu = \nu_{\text{Ising}} = 1 \Rightarrow \omega_{\nu,\text{Ising}} = 0.6 \pm 0.2, \tag{31}$$

indicative of an extremely slow rate of convergence toward asymptotic behavior. Using the corresponding values of $e_0(g_c)$, $q_0(g_c)$, and $s_0(g_c)$ as reference points, we find that convergence to asymptotic behavior, defined as a relative deviation of less than 1% from asymptotic values, would then be reached for $L \simeq O(10^5)$, or well beyond the reach of current computing power.

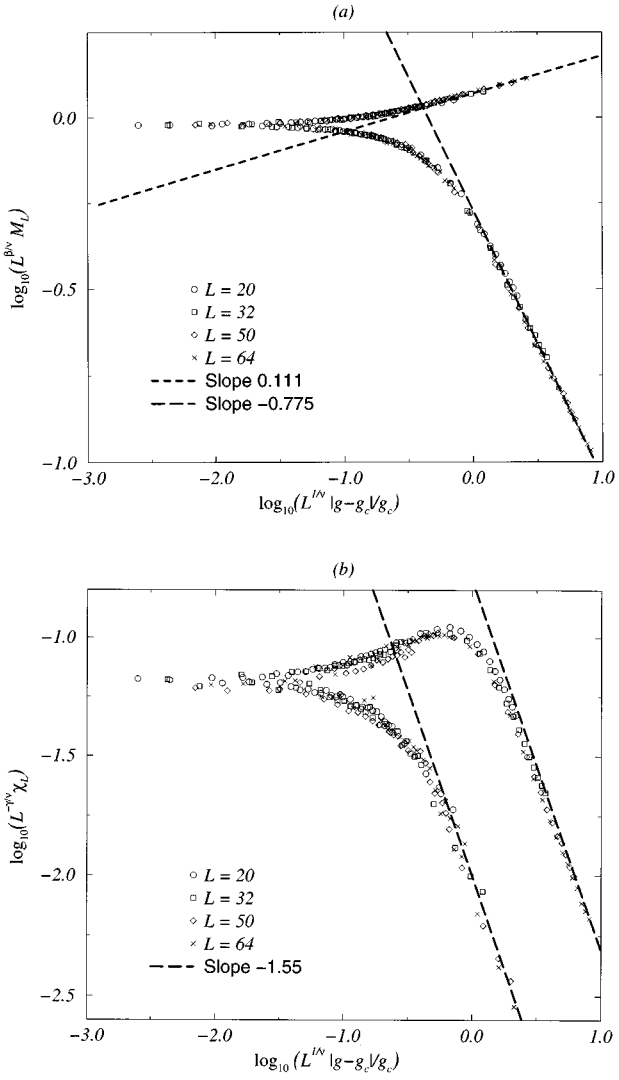

FIG. 11. Data collapses close to the continuous transition of Miller and Huse's model. The data are the same as in Fig. 5. Log-log plots of the reduced magnetization $L^{\beta/\nu}M_L$ [graph (a)] and susceptibility $L^{-\gamma/\nu}\chi_L$ [graph (b)] are presented vs the reduced control parameter $L^{1/\nu}|g-g_c|/g_c$ for numerical values $g_c = g_c^\infty = 0.205\,34$, $\beta/\nu = (\beta/\nu)_{\text{Ising}} = 0.125$, $\gamma/\nu = (\gamma/\nu)_{\text{Ising}} 1.75$, $\nu = 0.887$, and $20 \leqslant L \leqslant 64$. Note the good agreement of asymptotic behavior with the non-Ising exponent $\nu = 0.887$.

In addition, indirect support of the validity of estimates (30) is provided by collapses of magnetization and susceptibility data obtained for different system sizes. Neglecting corrections to scaling in Eq. (25), the following homogeneous forms are expected to apply:

$$L^{\beta/\nu} M_L(g) = \hat{M}((g-g_c^\infty)L^{1/\nu}),$$

$$L^{-\gamma/\nu}\chi_L(g) = \hat{\chi}((g-g_c^\infty)L^{1/\nu}). \tag{32}$$

The data sets previously presented in Fig. 5 ($L \leqslant 64$) yield excellent collapses for $\nu = 0.887$ [Eq. (28)], and the Ising values $\beta/\nu = 0.125$ and $\gamma/\nu = 1.75$ (Fig. 11). Interestingly, the large-size behavior of M_L and χ_L, as observed in log-log scale in the limit $|g-g_c^\infty|L^{1/\nu} \to \infty$, is consistent with straight lines of respective slopes $\beta = 0.111$, $-\gamma/2 = -0.775$, and

$-\gamma=-1.55$, in agreement with Eq. (30). The same estimates [Eq. (30)] are also consistent with relation (15), and deviate only slightly from values obtained directly from simulations of large-size systems [$L=1024$, Eq. (11)]. Note, however, that the quality of collapses obtained from Eq. (17) is similar for both $\nu=0.887$ and $\nu=\nu_{\mathrm{Ising}}=1$.

Numerical data presented in this section strongly suggest that the continuous transition of Miller and Huse's CML does *not* belong to the Ising universality class. Provided that the behavior observed for $L\leqslant 64$ meaningfully approximates the infinite-size limit behavior, our estimate of the correlation-length exponent, $\nu=0.887(18)$, is significantly lower than the expected $\nu_{\mathrm{Ising}}=1$. Yet a slow crossover to Ising behavior cannot be ruled out for very large system sizes. On the sole basis of data presented so far, our claim does not constitute a definite proof. Unfortunately, our analysis of corrections to scaling also shows that the sizes needed in order to provide a decisive numerical answer to this point lie far beyond present computing capabilities [$L\simeq O(10^5)$]. The true critical exponents of the transition, be they Ising or not, are naturally expected to be in some sense universal. The coming section is aimed at assessing the ''degree'' of universality of the non-Ising estimates (30).

III. RELEVANT PARAMETERS FOR NONEQUILIBRIUM UNIVERSALITY

The continuous phase transition first reported in [3] is by no means a unique phenomenon: Ising-like transitions are easily observed in coupled map lattices and related models [4], once a small number of conditions is fulfilled. The models investigated in this section share the following properties: the evolution rule is homogeneous, the local map is odd and chaotic. The lattice is two dimensional, and coupling between sites is short ranged. At the macroscopic level, an up-down symmetry is spontaneously broken in the ordered phase. These restrictions are inspired by the conditions which are known to define universality classes at equilibrium [23]. Our main goal here is to test whether or not the same conditions hold for far-from-equilibrium transitions of CML's (Sec. III A). Furthermore, the phase transition of a CML belonging to the same universality class as Miller and Huse's model may turn out to be free from (nonuniversal) corrections to dominant scaling, thus allowing a reliable estimate of the correlation-length exponent ν. We would also like to determine which features specific to CMLs may affect critical properties. In particular, the role played by bounded, deterministic local fluctuations and by synchronous update will be assessed (Secs. III B and III C, respectively).

All models discussed in Sec. III are simulated and analyzed according to the experimental protocol exposed in detail in Sec. II. Initial conditions are drawn at random over the CML's phase-space, boundary conditions are periodic. All regimes considered correspond to the unique (numerical) attractor of the system's dynamics. The largest system size is $L_{\max}=128$. The achieved statistical accuracy is of the same order for all models. Overall consistency in the measurement process allows meaningful comparison of exponent values, everywhere estimated by taking into account one effective corrective exponent (cf. Sec. II D). Note that macroscopic quantities exhibit the same scaling behavior, for the same critical exponents, when averaged over continuous local variables, as in

$$m^t_{\mathrm{cont},L}=\frac{1}{L^2}\sum_{i,j} x^t_{i,j}\,, \tag{33}$$

instead of local spins [cf. Eq. (6)]. Simulations reported in this article required about seven years of the CPU time of a DEC/Alpha processor running at 110 MHz. For brevity's sake, only figures related to the exponent ν are included, in practice figures similar to Figs. 8 and 9 of Sec. II. The interested reader is referred to [36] for additional details, and in particular for graphs leading to estimates of the critical points and of exponent ratios β/ν and γ/ν.

A. Testing universality within CML's

Static critical exponents of equilibrium second-order phase transitions of systems with short-range interaction only depend on the type of broken symmetry and on the space dimensionality. In this section, we consider extensively chaotic, purely deterministic, synchronously updated, two-dimensional CML's with an Ising-type ordering transition. The changes made on Miller and Huse's CML are known to be irrelevant at equilibrium: we first modify the local map (Sec. III A 1), then the coupling scheme (Sec. III A 2). The corresponding transitions are thus expected to belong to the same universality class.

1. Smooth local map

CML's which combine evolution rule (2) with an odd local map admitting three unstable fixed points do *not* necessarily exhibit an Ising-like phase transition [36]. In some cases, the CML remains paramagnetic for all parameter values. In others, a period-doubling transition is observed. Since the relationship linking microscopic dynamics and macroscopic ordering is unclear at present, our approach remains mostly empirical.

The first model we investigate is obtained by replacing the piecewise linear map of Miller and Huse's model [Eq. (4)] by a smooth, cubic map of the interval $[-1,1]$ (cf. Fig. 12),

$$f(x)=3x-4x^3, \tag{34}$$

while other features of the model are left unchanged. Since its map possesses both expanding and contracting parts. the corresponding coupled system, referred to as $C4$, may be thought of as more generic than Miller and Huse's model. Whereas the (one-dimensional) cubic map is conjugate to the piecewise linear map [Eq. (4)], and is therefore characterized by the same Lyapunov exponent, this property does not hold for the coupled system. Lattices of coupled cubic maps turn out to be less chaotic, as can be quantitatively shown, e.g., by numerical calculations of the Lyapunov spectra. Longer coherence times then translate into longer simulation times, for a given level of statistical accuracy.

An Ising-like transition, phenomenologically similar to that of Miller and Huse's CML, is observed at intermediate coupling strength g. The spatial extension of the intersection region of curves of Binder's cumulant $U_L(g)$ leads to an estimate of the critical coupling constant:

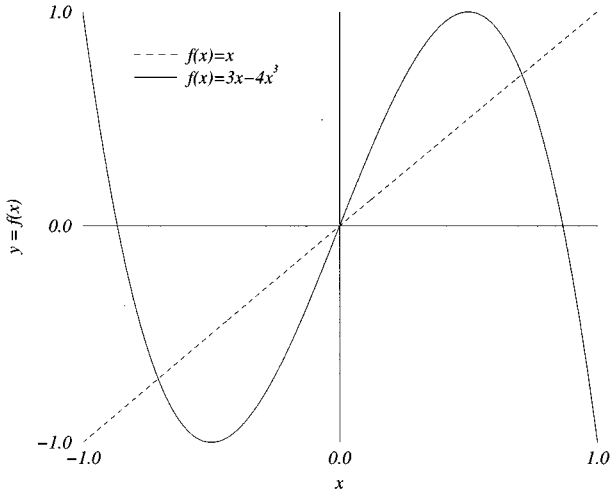

FIG. 12. A graph of the smooth, cubic local map used in model $C4$.

$$g_c^{\infty} = 0.178\,64(4),$$

$$-U^*(g_c^{\infty}) = 1.83(1). \tag{35}$$

This value of U^* is again compatible with the Ising estimate. The critical behavior is everywhere similar to that of Miller and Huse's model. Estimates of critical ratios and exponents, obtained from Eq. (35), are consistent with values (28) and (29):

$$\beta/\nu = 0.125(7),$$

$$\gamma/\nu = 1.75(4),$$

$$\nu = 0.91(4). \tag{36}$$

Values obtained from Eq. (36) for the exponents β and γ are given in Table I, in good agreement with Eq. (30). Convergence to Ising asymptotic behavior is rapid for both magnetization and susceptibility, as confirmed by large values of the corresponding corrective exponents $\omega_M \sim \omega_\chi \sim 5$. As before, strong corrections to scaling render the measurement of ν inconclusive (Fig. 13): the possibility of a slow relaxation toward Ising behavior, governed by a corrective exponent smaller than 1, cannot be ruled out.

Local maps defined on the whole real axis, such as Eq. (40), were also investigated. In all cases considered, preliminary results indicate that strong corrections to dominant scaling impair the evaluation of ν, while relaxation toward $\beta/\nu = (\beta/\nu)_{\text{Ising}}$ and $\gamma/\nu = (\gamma/\nu)_{\text{Ising}}$ is fast. This suggests that critical exponents are indeed insensitive to the choice of a local map, and that the presence of strong corrections to scaling for ν may in fact be related to the particular evolution rule used so far, i.e., to nearest-neighbor coupling on a square lattice.

2. Transition with weak corrections to scaling

The role played by the (short-range) evolution rule is investigated in this section. We focus on a CML defined by the combination of Miller and Huse's map [Eq. (4)] and a locally anisotropic evolution rule

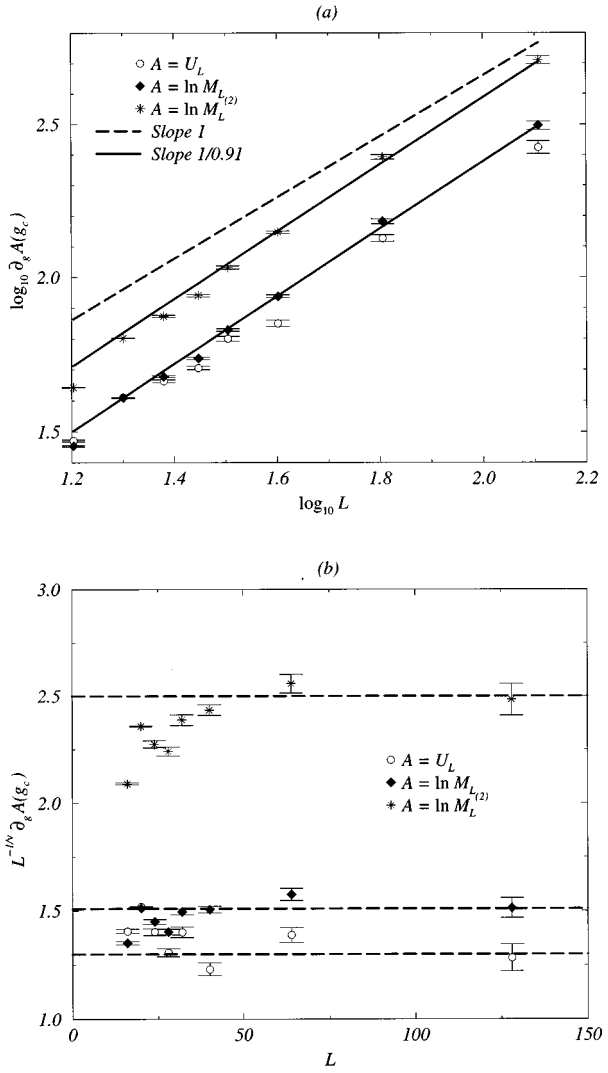

FIG. 13. Measure of the correlation-length exponent ν for the continuous transition of model $C4$ (cubic local map, four-nearest-neighbor coupling). A direct measure is obtained from graph (a), where quantities $\partial_g U_L(g_c)$, $\partial_g \ln M_L(g_c)$, and $\partial_g \ln M_L^{(2)}(g_c)$ are plotted vs L on a log-log scale at the critical point $g = g_c^{\infty} = 0.17864(4)$. Our best estimate ($\nu = 0.91$) is tested in graph (b), presenting $\partial_g U_L(g_c)/L^{1/\nu}$, $\partial_g \ln M_L(g_c)/L^{1/\nu}$, and $\partial_g \ln M_L^{(2)}(g_c)/L^{1/\nu}$ vs L on a lin-lin scale.

$$x_{2i,j}^{t+1} = (1-3g) f(x_{2i,j}^t) + g\big(f(x_{2i-1,j}^t) + f(x_{2i+1,j}^t) + f(x_{2i,j+1}^t)\big),$$

$$x_{2i+1,j}^{t+1} = (1-3g) f(x_{2i+1,j}^t) + g\big(f(x_{2i,j}^t) + f(x_{2i+2,j}^t) + f(x_{2i+1,j-1}^t)\big) \tag{37}$$

referred to as MH3. Rule (37) is defined on a two-dimensional square lattice of Cartesian indices (i,j), and applied synchronously to all lattice sites. Each site is coupled to three of its nearest neighbors: sites belonging to even (odd) columns of the lattice are coupled vertically to their northern (southern) neighbor only. The coupling constant g thus belongs to the interval $[0, \frac{1}{3}]$. An Ising-like phase transition

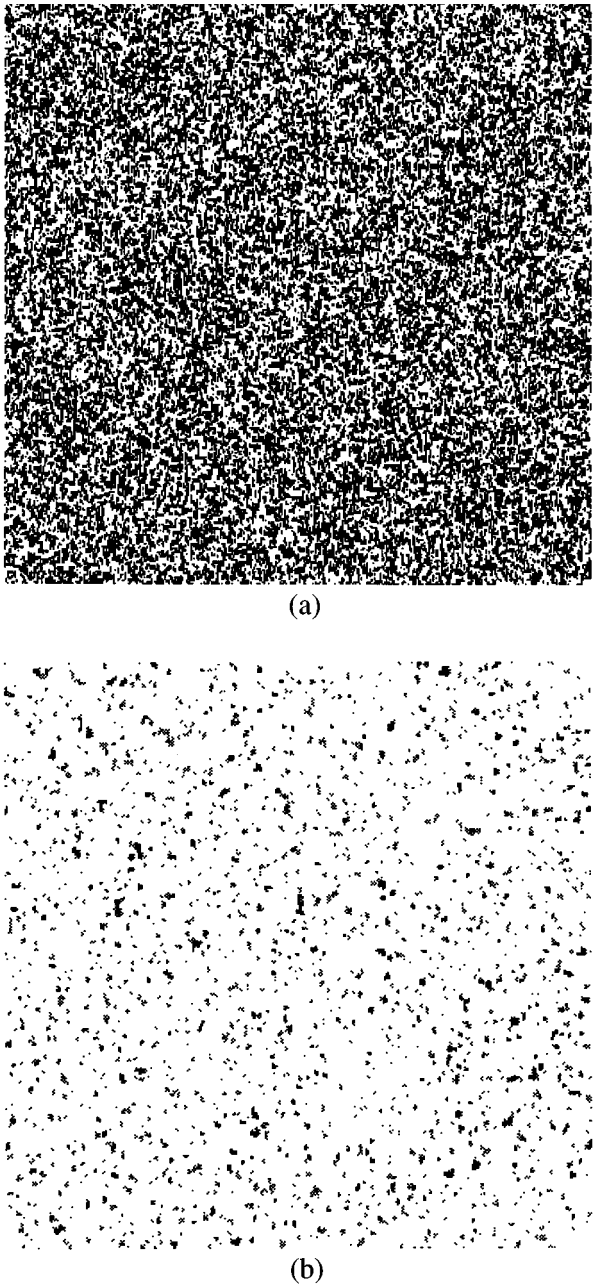

FIG. 14. Typical snapshots of model MH3 (locally anisotropic evolution rule) taken in the time-asymptotic regime far from criticality [$g_c^\infty = 0.25118(4)$]. Up- and down-spins are represented by black and white pixels, respectively. (a) Disordered phase, $g = 0.18$. (b) Ordered phase, $g = 0.28$. The system size is $L = 400$.

occurs for a critical coupling $g_c \sim 0.25$. The *local* anisotropy of rule (37) is erased at large scales, where patterns are isotropic (Fig. 14).

Since a unique correlation length ξ can be defined, and shown to diverge at criticality, we expect the finite-size scaling laws discussed in Sec. II to apply. Accordingly, Binder's method leads to an estimate of the critical coupling constant

$$g_c^\infty = 0.251\ 18(4),$$

$$-U^*(g_c^\infty) = 1.823(3), \tag{38}$$

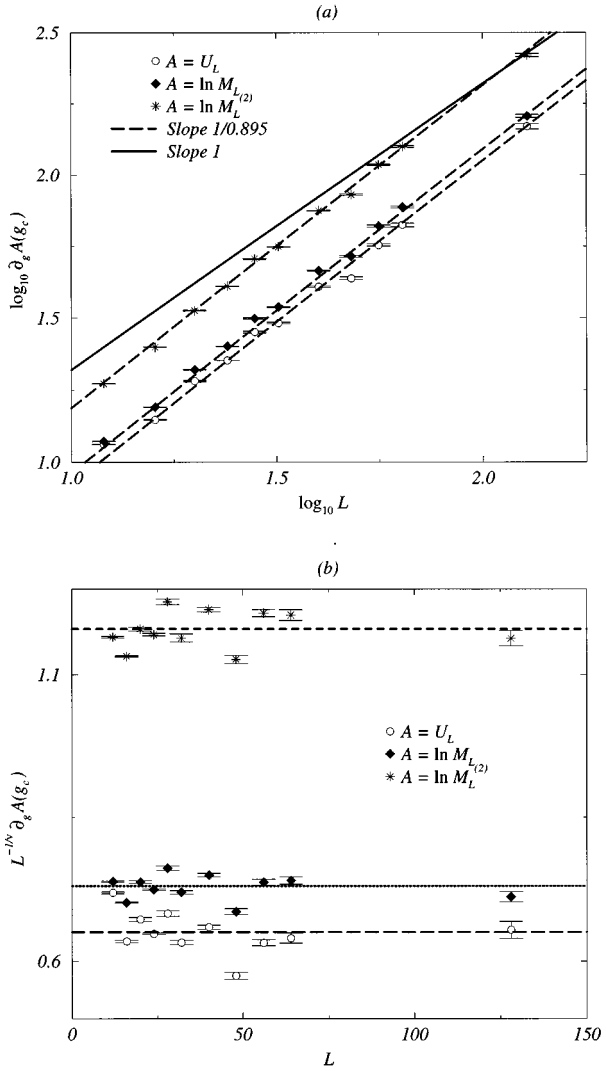

FIG. 15. Measure of the correlation-length exponent ν for the continuous transition of model MH3 (piecewise-linear local map, three nearest-neighbor, locally anisotropic coupling). The quantities plotted are the same as described in Fig. 13, for the relevant numerical values $g = g_c^\infty = 0.251\ 18(4)$, $\nu = 0.895$. Notice the absence of corrections to scaling in graph (b).

where the estimated cumulant is slightly lower than its Ising value. We find values of critical quantities:

$$\beta/\nu = 0.131(6),$$

$$\gamma/\nu = 1.73(3),$$

$$\nu = 0.895(12) \tag{39}$$

for corrective exponents $\omega_M \sim \omega_\chi \sim 5$. A crucial observation is that corrections to dominant scaling are suppressed for the quantities $\partial_g U_L(g_c^\infty)$, $\partial_g \ln M_L^{(2)}(g_c^\infty)$ and $\partial_g \ln M_L(g_c^\infty)$ (cf. Fig. 15). Convergence to asymptotic behavior is already achieved for the smallest size considered, $L = 12$. This feature justifies the somewhat unusual choice of rule (37). The numerical value $\nu = 0.895(12)$ given in Eq. (39) is obtained from straightforward linear fits of the data presented in Fig. 15, over the whole range of available sizes ($12 \leqslant L \leqslant 128$). We

can thus safely conclude that this transition does *not* belong to the Ising universality class, since its correlation exponent ν is *not* consistent with $\nu_{\mathrm{Ising}}=1$.

Table I sums up the numerical values of critical exponents of models MH4, C4, and MH3. Since excellent mutual agreement is achieved, and since critical exponents are in principle insensitive to microscopic details of the CML, such as the choice of the local map or local coupling, our data strongly suggest that the three transitions belong to a unique universality class, characterized by a correlation-length exponent significantly lower than the Ising value. In other words, we now feel confident that the estimates of ν derived in Secs. II D and III A 1 from the scaling behavior of systems of small sizes are in fact equal to values pertaining to the infinite-size limit. Note that we have no specific understanding as to why implementing evolution rule (37) happens to suppress corrections to scaling. In particular, strong corrections to scaling are again observed in the nearby case of nearest-neighbor coupling on a honeycomb lattice. The coupling scheme (37) may thus constitute a fortunate, yet isolated case.

B. Noise-driven phase transitions

Phase transitions of two-dimensional, extensively-chaotic CML's, which were expected to belong to the Ising universality class on rather general grounds, turn out to exhibit universal, yet distinctly non-Ising critical behavior. For one-dimensional CML's, it was recently argued that the nonuniversal behavior of phase transitions akin to directed percolation may be related, below threshold, to the inherent complexity, and thus to the ''imperfect'' character of deterministic fluctuations produced by chaotic dynamical systems [13]. In the context of nonequilibrium growth phenomena, roughening exponents of nonlinear, stochastic partial differential equations subjected to colored noise are known to vary continuously with the value of the exponent governing the tail of the noise distribution [37]. It is thus natural to wonder whether the unexpected critical properties reported above may be connected to the particular nature of the deterministic, bounded fluctuations generated by chaotic maps.

This question is now addressed, by investigating the critical properties of noise-driven phase transitions of stochastic CML's. When subject to an external, unbounded, white noise, the local phase space of each individual map must nonetheless remain invariant under the CML's evolution rule. For that reason, we opt for an odd, chaotic map defined on the whole real axis as (cf. Fig. 16)

$$f(x)=\lambda(x-x^3)\exp(-x^2), \tag{40}$$

and characterized by three unstable fixed points for large enough values of its real parameter λ. The exponential in Eq. (40) ensures that the CML's attracting set remains bounded.

1. Four-neighbor coupling

Map (40) is first implemented on a square lattice with nearest-neighbor coupling. The evolution rule of the resulting synchronously-updated, stochastic CML reads

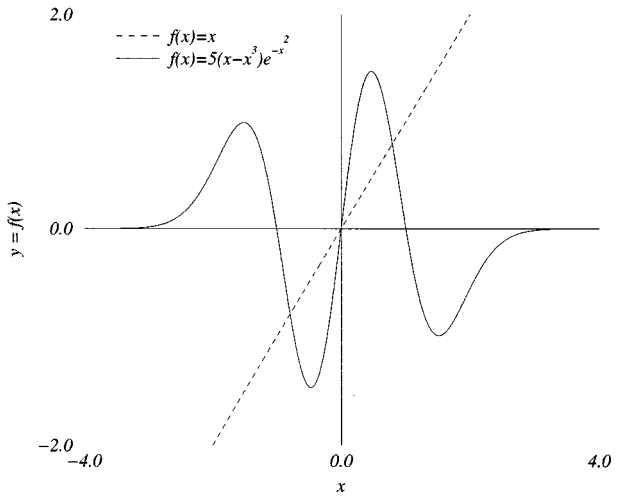

FIG. 16. A graph of the smooth, local map used in stochastic models $N4$ and $N3$.

$$x_{i,j}^{t+1}=(1-4g)f(x_{i,j}^t)+g\big(f(x_{i-1,j}^t)+f(x_{i,j-1}^t)+f(x_{i+1,j}^t)+f(x_{i,j+1}^t)\big)+\eta_{i,j}^t, \tag{41}$$

where $\eta_{i,j}^t$ denotes Gaussian, white noise with the following correlation functions:

$$\langle \eta_{i,j}^t \eta_{k,l}^{t'}\rangle = 2D\,\delta(i-k)\,\delta(j-l)\,\delta(t-t'). \tag{42}$$

Sequences of uncorrelated pseudorandom numbers are produced by a generator of Fibonacci type, with a period much longer than the $O(10^{11})$ numbers needed for the largest sizes considered. Their distribution is made Gaussian by a standard Box-Müller-type algorithm. We checked that our results are not altered by a different choice of random-number generator.

Three control parameters are in principle available: the coupling strength g, the map's parameter λ, and the noise intensity D. The value of λ is first set so that the corresponding pure CML [evolution rule (2)] undergoes a coupling-driven Ising-like transition for an intermediate value of g. The coupling constant is next chosen in a range compatible with the existence of a ferromagnetic phase. For the same fixed set of parameter values (λ,g), a noise-driven Ising-like transition occurs under evolution rule (41) for a critical noise intensity D_c. Strong enough external noise, somewhat similar to the temperature of equilibrium systems, destroys long-range order and leads to a paramagnetic phase $(D\geqslant D_c)$.

For the *fixed set* of parameter values $(\lambda,g)=(5.0,0.22)$, the locus of an Ising-like phase transition can be circumscribed to the region defined by

$$D_c^{\infty}=0.018\,05(15),$$
$$-U^*(D_c^{\infty})=1.834(13) \tag{43}$$

by applying Binder's method on numerical data obtained for sizes $12\leqslant L\leqslant 64$ only, due to the additional numerical cost of drawing random numbers. Good agreement with the Ising value of U^* is again observed. The status of critical quantities is similar to that obtained for models previouly defined

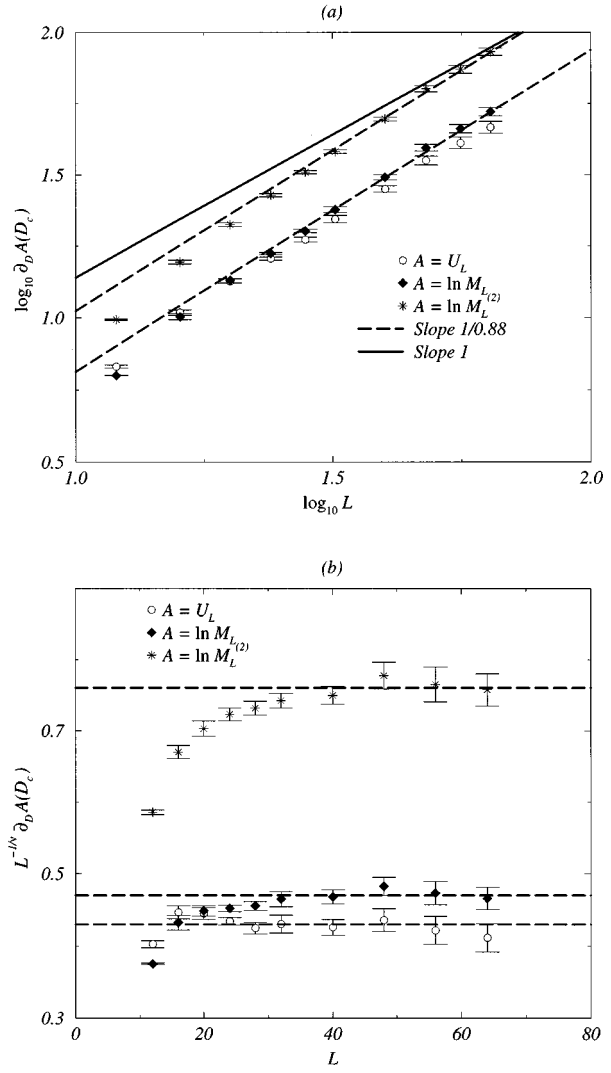

FIG. 17. Measure of the correlation-length exponent ν for the noise-driven continuous transition of stochastic CML $N4$ (local map defined over the whole real axis, nearest-neighbor coupling). The quantities plotted are analogous to quantities described in Fig. 13, for the relevant numerical values $D=D_c^{\infty}=0.018\,05(15)$, $\nu=0.88$. Graph (b) shows the presence of strong corrections to dominant scaling.

on a square lattice with nearest-neighbor coupling, as described in Secs. II and III A 1. Our estimates are

$$\beta/\nu=0.122(6),$$

$$\gamma/\nu=1.70(4),$$

$$\nu=0.88(6) \tag{44}$$

for effective corrective exponents equal to $\omega_M=6(1)$, $\omega_\chi=2.6(1)$, and $\omega_\nu=5.5(1.0)$. While good agreement with Ising values is easily obtained for exponent ratios β/ν and γ/ν, strong corrections to dominant scaling (cf. Fig. 17) as well as larger than usual error bars hinder a straightforward evaluation of ν. Values of the critical exponents β, γ, and ν are listed in Table II, under the heading $N4$. Preliminary results on other noise-driven transitions of stochastic CML's obeying evolution rule (41), for different choices of parameters (λ,g), as well as on *coupling*-driven phase transitions observed when varying g for fixed parameter values (λ,D), suggest that the intensity of corrections to scaling is rather insensitive to the particular choice of model, provided that the evolution rule involves nearest-neighbor coupling on a square lattice.

TABLE II. Critical exponents of synchronously updated, stochastic CML's. Abbreviations MH4, $N4$, and $N3$ correspond respectively to Miller and Huse's model and to the noisy CML's discussed in Secs. III B 1 and III B 2, defined by nearest-neighbor and locally anisotropic three-neighbor coupling schemes. The three transitions belong to the same (non-Ising) universality class.

	MH4	$N4$	$N3$
$g_c^{\infty}/D_c^{\infty}$	0.205 34(2)	0.018 05(15)	0.023 66(6)
$-U^*$	1.832(4)	1.834(13)	1.830(6)
β/ν	0.125(4)	0.122(6)	0.126(7)
γ/ν	1.748(10)	1.70(4)	1.752(11)
$(2\beta+\gamma)/\nu$	2.00(2)	1.95(6)	2.00(3)
β	0.111(5)	0.108(13)	0.113(9)
γ	1.55(4)	1.50(14)	1.56(5)
ν	0.887(18)	0.88(6)	0.89(2)

2. Three-neighbor coupling

We now consider a variation on evolution rule (37), modified so as to include additive white noise. The resulting noisy CML, denoted hereafter as $N3$, is defined on a square lattice as follows:

$$x_{2i,j}^{t+1}=(1-3g)f(x_{2i,j}^{t})+g\big(f(x_{2i-1,j}^{t+1})+f(x_{2i+1,j}^{t})+f(x_{2i,j+1}^{t})\big)+\eta_{2i,j}^{t},$$

$$x_{2i+1,j}^{t+1}=(1-3g)f(x_{2i+1,j}^{t})+g\big(f(x_{2i,j}^{t+1})+f(x_{2i+2,j}^{t})+f(x_{2i+1,j-1}^{t+1})\big)+\eta_{2i+1,j}^{t}, \tag{45}$$

where $\eta_{i,j}^{t}$ denotes δ-correlated Gaussian noise [cf. Eq. (42)], and the function f is the map (40). Since the corresponding deterministic CML remains paramagnetic for all values of the coupling strength when $\lambda=5$, we choose to set the two control parameters to the values: $(\lambda,g)=(4.5,0.25)$. The deterministic limit $D=0$ corresponds to an ordered, ferromagnetic phase. A noise-driven Ising-like phase transition is observed for a noise intensity $D\geqslant D_c$ strong enough to destabilize this regime. Since no trace of the microscopic anisotropy present in rule (45) is left at large enough length scales, we safely turn to the same finite-size scaling laws in order to estimate the critical quantities of this transition.

Numerical data obtained from simulations of finite-size systems $(8\leqslant L\leqslant 64)$ lead to the following estimate of the critical noise intensity:

$$D_c^{\infty}=0.023\,66(6),$$

$$-U^*(D_c^{\infty})=1.830(6), \tag{46}$$

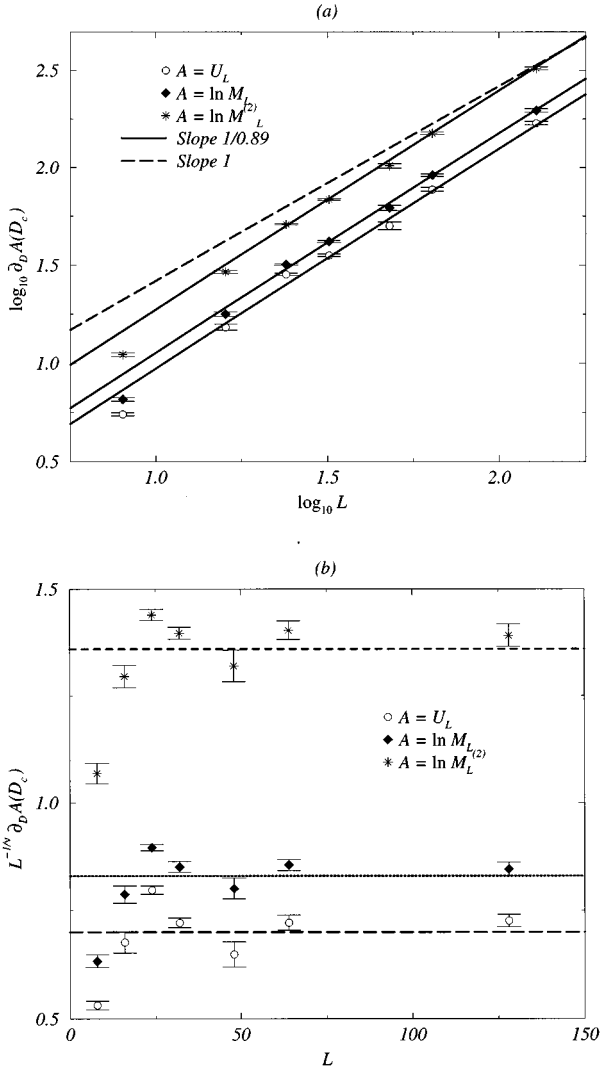

FIG. 18. Measure of the correlation-length exponent ν for the noise-driven continuous transition of stochastic CML $N3$ (local map defined over the whole real axis, three nearest-neighbor, locally anisotropic coupling). The quantities plotted are analogous to quantities described in Fig. 13, for the relevant numerical values $D=D_c^{\infty}=0.02366(6)$, $\nu=0.89$. As before, corrections to scaling are suppressed by the implementation of three-neighbor, locally anisotropic coupling.

where the value of Binder's cumulant at criticality is in good agreement with the Ising result. The corresponding exponent ratios are

$$\beta/\nu=0.126(7),$$

$$\gamma/\nu=1.752(11),$$

$$\nu=0.89(2) \tag{47}$$

obtained for corrective exponents equal to $\omega_M=2.5(7)$ and $\omega_\chi=2.2(1)$. However, rule (45) suppresses corrections to dominant finite-size scaling of the quantities $\partial_D U_L(D_c^{\infty})$, $\partial_D \ln M_L^{(2)}(D_c^{\infty})$ and $\partial_D \ln M_L(D_c^{\infty})$: relaxation to asymptotic behavior is clearly achieved as soon as $L=16$ (Fig. 18).

Exponents β, γ, and ν, listed in Table II under the heading $N3$, are not compatible with the Ising universality class. Since models $N4$ (Sec. III B 1) and $N3$ (this section) are expected to belong to the same universality class, we believe that the previous estimates (44) do indeed correspond to infinite-size, asymptotic behavior. Moreover, good agreement is achieved between the present values (47) and those already obtained for Miller and Huse's CML with four- and three-neighbor coupling [Eqs. (30) and (39)]. We conclude that the nature of the microscopic fluctuations generated by CML's is *not* a relevant parameter for critical exponents of Ising-like phase transitions of CML's. This is in a sense mildly surprising: we already showed in Secs. II and III A that transitions of deterministic CML's using different maps [Eqs. (4), (34), and (40)], and thus characterized by different invariant measures, do belong to the same universality class. This section generalizes this first, and until now implicit, result to the (generic) case of unbounded local fluctuations.

C. Deterministic, asynchronously updated models

Equilibrium stochastic systems, such as the Ising model, can be simulated numerically thanks to the Monte Carlo algorithm, which ensures that the system's phase space is sampled according to its invariant measure. Spins are usually updated asynchronously, in practice one at a time, the precise order of update being irrelevant. Even though intermediate situations, e.g., simultaneous update of appropriately defined clusters of spins [38], were considered in order to speed up simulations, it is generally believed that equilibrium spin systems such as the Ising model cannot be simulated by synchronous algorithms [39], at least for cellular automata with discrete phase space. Furthermore, simulations of Langevin equations, such as Eq. (1), also respect asynchronous numerical schemes. Since such equations form the backbone of theoretical arguments ruling out non-Ising critical behavior in Ising-like transitions of CML's [26,27], it is natural to ask whether a so far largely unnoticed, yet fundamental distinction between synchronously and asynchronously updated systems may not lie of the origin of the non-Ising behavior reported here.

In this section, we attempt to determine whether synchronous update is the relevant parameter responsible for the reported deviation from Ising universality. We consider variations of Miller and Huse's model obtained by updating lattice sites one by one. An asynchronous update can of course be implemented in a number of different ways. For simplicity's sake, we focus here on a fixed, sequential update. In practice, we choose to update the (square) lattice's rows one after another, and sites within the same row following their column's index. A pictorial representation is given by the following graph:

$$\cdots\rightarrow(1,1)\rightarrow(2,1)\rightarrow(3,1)\rightarrow\cdots\rightarrow(L,1)\rightarrow$$

$$\rightarrow(1,2)\rightarrow(2,2)\rightarrow(3,2)\rightarrow\cdots\rightarrow(L,2)\rightarrow$$

$$\cdots$$

$$\rightarrow(1,L)\rightarrow(2,L)\rightarrow(3,L)\rightarrow\cdots\rightarrow(L,L)\rightarrow\cdots, \tag{48}$$

where arrows indicate the order of update between sites of indices (i,j), helical boundary conditions being used when linking two consecutive rows. Other asynchronous schemes may involve, for instance, the random choice of each updated site over the lattice, where disorder may be either annealed or frozen. Such choices are left for future study. We believe that results presented in this section are of a general nature, and do not depend on the type of asynchronous update implemented in practice.

1. Four-neighbor coupling

We first choose to implement Miller and Huse's CML with nearest-neighbor coupling on a square lattice according to the fixed, sequential, site by site update rule described above. For periodic boundary conditions, rule (2) now assumes the form

$$x_{i,j}^{t+1}=(1-4g)f(x_{i,j}^{t})+g\big(f(x_{i-1,j}^{t+1})+f(x_{i,j-1}^{t+1})+f(x_{i+1,j}^{t}) + f(x_{i,j+1}^{t})\big). \tag{49}$$

The local map is left unchanged [cf. Eq. (4)], the unique control parameter is the coupling constant $g\in[0,\frac{1}{4}]$.

An Ising-like transition occurs at

$$g_c^{\infty}=0.112\,55(5),$$
$$-U^{*}(g_c^{\infty})=1.835(14), \tag{50}$$

as estimated according to Binder's method for systems sizes smaller than $L=64$, a limit imposed by the larger than usual coherence times present in this system. An asynchronous update turns out to stabilize the ferromagnetic phase: the critical coupling (50) is much lower than that estimated in the synchronous case, Eq. (19). We find that convergence to *Ising* critical behavior is achieved as soon as $L\sim 20$ (cf. Fig. 19). The estimated critical exponents are

$$\beta/\nu=0.117(12),$$
$$\gamma/\nu=1.76(5),$$
$$\nu=1.02(7) \tag{51}$$

for (large) corrective exponents $\omega_M=6(2)$, $\omega_\chi=3.0(1)$, and $\omega_\nu=4.5(1.5)$. Estimates of exponents β, γ and ν are given in Table III, under the heading MH4 Async., and fully agree with Ising exponents. This suggests that synchronous update is indeed relevant in the renormalization group sense.

2. Three-neighbor coupling

In order to check the robustness of this first result, we naturally turn to an asynchronously-updated version of locally anisotropic rule (37). Once adapted to site by site, sequential update, its evolution rule reads

$$x_{2i,j}^{t+1}=(1-3g)f(x_{2i,j}^{t})+g\big(f(x_{2i-1,j}^{t+1})+f(x_{2i+1,j}^{t}) + f(x_{2i,j+1}^{t})\big),$$
$$x_{2i+1,j}^{t+1}=(1-3g)f(x_{2i+1,j}^{t})+g\big(f(x_{2i,j}^{t+1})+f(x_{2i+2,j}^{t}) + f(x_{2i+1,j-1}^{t+1})\big), \tag{52}$$

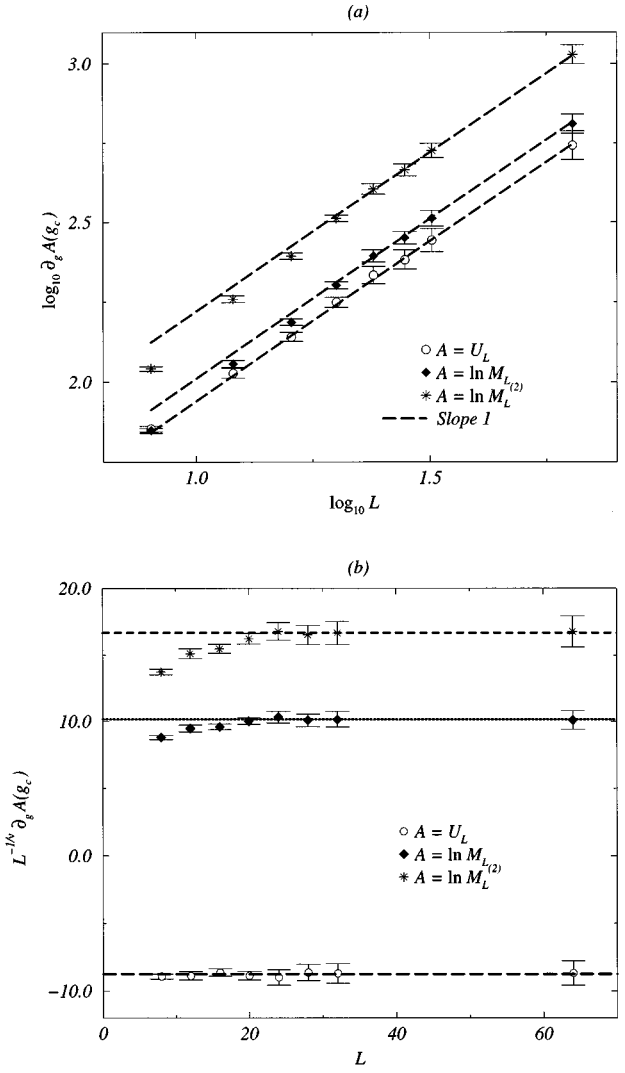

FIG. 19. Measure of the correlation-length exponent ν for the coupling-driven continuous transition of asynchronously-updated model MH4 Async. (piecewise-linear local map, nearest-neighbor coupling). The quantities plotted are analogous to quantities described in Fig. 13, for the relevant numerical values $g=g_c^{\infty}=0.11255(5)$, $\nu=\nu_{\mathrm{Ising}}=1$. Convergence to Ising behavior is achieved as soon as $L=20$.

where periodic boundary conditions are used, and the coupling constant g belongs to the interval $[0,\frac{1}{3}]$.

According to numerical data obtained for system sizes smaller than $L_{\max}=128$, a transition is observed at

$$g_c^{\infty}=0.158\,47(2),$$
$$-U^{*}(g_c^{\infty})=1.832(12) \tag{53}$$

for a critical coupling constant much lower than measured in the synchronous case [Eq. (38)]. Critical exponents are again in good agreement with Ising values,

$$\beta/\nu=0.124(13),$$
$$\gamma/\nu=1.72(1),$$
$$\nu=0.99(4), \tag{54}$$

TABLE III. Critical exponents of asynchronously-updated models. Abbreviations MH4, MH4 Async., and MH3 Async. correspond respectively to Miller and Huse's model and to the asynchronously updated models discussed in Secs. III C 1 and III C 2, defined by nearest-neighbor and locally anisotropic three-neighbor coupling schemes. Ising-like transitions of asynchronously updated models belong to the Ising universality class.

	MH4	MH4 Async.	MH3 Async.
g_c^∞	0.205 34(2)	0.112 55(5)	0.158 47(2)
$-U^*$	1.832(4)	1.835(14)	1.832(12)
β/ν	0.125(4)	0.117(12)	0.124(13)
γ/ν	1.748(10)	1.76(5)	1.72(1)
$(2\beta+\gamma)/\nu$	2.00(2)	2.01(8)	1.96(3)
β	0.111(5)	0.126(27)	0.123(18)
γ	1.55(4)	1.79(17)	1.71(9)
ν	0.887(18)	1.02(7)	0.99(4)

except for exponent ratio γ/ν, slightly lower than expected. The corresponding corrective exponents are $\omega_M = 2.2(4)$ and $\omega_\chi = 2(1)$. The quantities $\partial_g U_L(g_c^\infty)$, $\partial_g \ln M_L(g_c^\infty)$, and $\partial_g \ln M_L^{(2)}(g_c^\infty)$ reach an asymptotic scaling regime consistent with the Ising universality class for $L \sim 32$ (cf. Fig. 20). Numerical estimates of exponents β, γ, and ν are listed in Table III, under the heading MH3 Async. Note that the combination of error bars on γ/ν and ν leads to a value of γ consistent with $\gamma_{\text{Ising}} = \frac{7}{4}$.

Consistency between exponents (51) and (54) confirms once more that critical properties do not depend on the particular choice of a microscopic evolution rule. Furthermore, analysis of numerical simulations of models MH4 Async. and MH3 Async. suggest that Ising-like transitions of asynchronously updated lattices of locally coupled chaotic maps belong to the Ising universality class. In other words, a synchronous update appears to be the relevant parameter responsible for the deviation from Ising universality observed in lattices of coupled chaotic maps.

Asynchronously updated models with adequate microscopic symmetry provide interesting ways to simulate the Ising model without having recourse to a pseudo-random-number generator. The achieved numerical efficiency is however rather poor, since local variables are continuous. Recent work by Sakaguchi [2] showed that the Ising model can also be implemented exactly thanks to a semisynchronous update scheme, where two checkerboard sublattices of a two-dimensional, square lattice of locally coupled Bernoulli maps are updated one after the other. Since this model respects a detailed balance, and is characterized by a Gibbs invariant measure, its critical exponents are exactly known to be equal to their Ising values, a point that we checked by numerical simulations analyzed as before. This further suggests that synchronous update of *all* lattice sites may well be an isolated case within the spectrum of possible update schemes: an asynchronous update decomposed on two sublattices suffices in order to restore Ising universality.

IV. DISCUSSION

Ising-like, chaos-to-chaos phase transitions of coupled map lattices are well described by scaling and finite-size scaling laws valid at equilibrium. This confirms indirectly that symmetry and ergodicity breaking, as signaled by the divergence of the system's (unique) correlation length, occur in the infinite-size limit. As for equilibrium systems, the numerical value of critical exponents which govern scaling laws is insensitive to microscopic details of the model, such as the choice of a local map or evolution rule. Our main result is that the nature of update is a relevant parameter: continuous transitions of two-dimensional, synchronously-updated CML's with an Ising-like, discrete broken symmetry form a new universality class. On the other hand, transitions of asynchronously updated models belong to the equilibrium Ising universality class. Interestingly, the nature of local fluctuations—deterministic or stochastic—turns out to be irrelevant.

Deriving accurate numerical estimates of critical exponents of deterministic systems is a notoriously difficult task

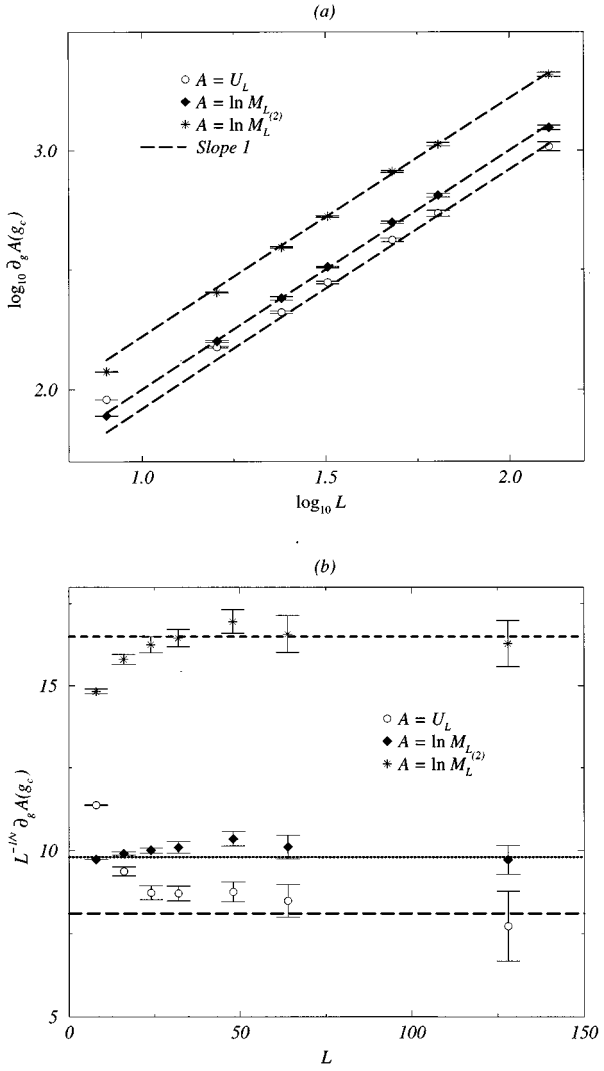

FIG. 20. Measure of the correlation-length exponent ν for the coupling-driven continuous transition of asynchronously-updated model MH3 Async. (piecewise-linear local map, three-nearest-neighbor, locally anisotropic coupling). The quantities plotted are analogous to quantities described in Fig. 13, for the relevant numerical values $g = g_c^\infty = 0.158\,47(2)$, $\nu = \nu_{\text{Ising}} = 1$. Convergence to Ising behavior is achieved for $L \sim 32$.

[6,12,13]. We believe that the methodology followed here is reliable for two main reasons: corrections to dominant scaling are taken into account and quantified; estimates of critical exponents are always derived from at least two transitions belonging *a priori* to the same universality class. The latter point suggests that systematic errors of an unknown nature do not bias our estimates. According to our simulations, the universality class of synchronously-updated models is characterized by the exponents

$$\beta = 0.115(9),$$

$$\gamma = 1.55(5),$$

$$\nu = 0.89(2) \tag{55}$$

obtained when combining error bars of estimates pertaining to the three models MH4, MH3, and $N3$, chosen for the (highest) quality of their data. Narrower error bars, which still lie within confidence intervals (55), can be obtained for exponents β and γ when giving credit to exact Ising values for exponent ratios β/ν and γ/ν, while retaining the numerical estimate $\nu = 0.89(2)$. Note that synchronous update does not affect the value of Binder's cumulant, nor the validity of the hyperscaling relation (cf. Tables I, II, and III)

$$2\beta + \gamma = \nu d \tag{56}$$

known to hold at equilibrium in the case of fluctuation-dominated transitions [23]. Preliminary results suggest that Eq. (56) may also hold in the case of transitions of three-dimensional hypercubic lattices, an observation compatible with a value of the upper critical dimension equal to $d_c = 4$ for Ising-like transitions of CML's [26,27].

The notion of *weak universality*, as introduced by Suzuki in the context of equilibrium critical phenomena [40], may provide a useful basis in order to account for exponent values (55). A number of exactly solved equilibrium models, such as Baxter's eight-vertex model [41], are known to exhibit anomalous, nonuniversal critical behavior, characterized by a continuous variation of critical exponents with parameters of the model which are in principle irrelevant. However, the *ratios* β/ν, γ/ν and $\hat{\phi} = (2-\alpha)/\nu$ respect Ising behavior. Suzuki noticed that, close to the transition point, the magnetization and susceptibility depend on the correlation length ξ according to the scaling laws

$$M \sim \xi^{-\beta/\nu},$$

$$\chi \sim \xi^{\gamma/\nu}, \tag{57}$$

while the singular part of the free energy behaves as

$$f_s \sim \xi^{-(2-\alpha)/\nu}. \tag{58}$$

Only quantities defined with respect to ξ remain universal in the case of Baxter's model, while usual exponents, defined with respect to the temperature difference from criticality $(T - T_c)$, depend on details of the model. For this reason, the—intrinsically defined—correlation length seems better apt at quantifying departure from criticality, and thus critical phenomena, than does an external control parameter such as the temperature. Weak universality denotes the independence of correlation-length-related exponents, such as β/ν, γ/ν, and $\hat{\phi}$, on microscopic details of the model [40]. In this sense, Baxter's model belongs to the *weak* universality class of the Ising model.

Even though Baxter's eight-vertex model admittedly represents a nongeneric, exceptional case [42], we would like to assess the relevance of Suzuki's weak universality to nonequilibrium, Ising-like transitions of CML's. In fact, weak universality is systematically tested by finite-size scaling methods. For systems whose finite-size correlation length ξ_L scales with L at criticality,

$$\xi_L \sim_{g \to g_c^\infty} L, \tag{59}$$

the scaling laws for finite-size quantities,

$$M_L \sim L^{-\beta/\nu},$$

$$\chi_L \sim L^{\gamma/\nu}, \tag{60}$$

closely parallel Eqs. (57). Finite-size scaling estimates of critical exponents β and γ depend on an independent measure of ν [32]. Furthermore, the ratio $\hat{\phi}$ can be expressed at equilibrium as

$$\hat{\phi} = (2\beta + \gamma)/\nu \tag{61}$$

by taking advantage of the scaling relation $\alpha + 2\beta + \gamma = 2$. Even though a proper definition of exponent α still lacks in far-from-equilibrium CML's, it is tempting to link the validity of the hyperscaling relation (56) to an hypothetical relation (58), which may relate the behavior of some coarse-grained free energy to the correlation length at criticality.

More importantly, the control parameters we consider, coupling strength g and noise intensity D, are defined at the microscopic level of evolution rules. They were chosen on an *ad hoc* basis, without particular theoretical grounding: attempts to define a meaningful, macroscopic ''temperature'' for extensively chaotic dynamical systems remain in their infancy [10,11]. We explicitly chose to define the continuous transition of a CML as a point in parameter space where the (well-defined, macroscopic) correlation length ξ_L diverges in the thermodynamic limit. These remarks justify the choice of the inverse correlation length ξ^{-1} as a more natural quantifier of departure from criticality than, say, the reduced coupling constant $(g - g_c)/g_c$. In a renormalization-group context, we tentatively introduced in [5] a distinction between scaling exponents y_B and y_T [cf. Eq. (12)], where $y_B = (\beta + \gamma)/\nu$ is ''superuniversal,'' while $y_T = 1/\nu$ depends on the type of update. This statement can now be rephrased in somewhat more appropriate terms as follows: while synchronous update defines a new (''strong'') universality class, all Ising-like transitions of CML's belong to the weak universality class of the two-dimensional Ising model, for both synchronous and asynchronous updates.

Quantities independent of the choice of a control parameter remain universal within a given weak universality class [40]. Indeed, our analysis shows that Binder's cumulant U^*, a quantity measured *at* criticality, is update independent. We conjecture that the critical exponent η, which governs the algebraic decay of the spatial correlation function at the

transition point, retains its Ising value for transitions of synchronously updated models: $\eta = \eta_{\text{Ising}} = \frac{1}{4}$. The same remark also applies to a so far hypothetical exponent $\delta = \delta_{\text{Ising}} = 15$, once appropriately defined from the response of the CML's order parameter to an external field. Estimating η and δ from numerical simulations may provide a direct test of our weak universality hypothesis. This is left for future study.

To conclude, we would like to briefly discuss a number of open questions raised by the present work. First of all, the existence of a nontrivial universality class of transitions of synchronously updated models represents a challenging theoretical puzzle, since it questions the applicability of two well-established tools—nonlinear Langevin equations and dynamic renormalization-group methods—to a new and largely unexplored context. One possible interpretation of this discrepancy is that asynchronously updated stochastic equations may not adequately describe the large-scale properties of extensively chaotic dynamical systems close to critical points, i.e., nongeneric points where the synchronous nature of update is felt up to macroscopic length scales, as shown by the anomalous value of exponent ν. Generalizing spin-block renormalization methods to extended dynamical systems may help building an appropriate, synchronously updated, coarse-grained description of CML's close to criticality.

While the scope of our investigations was deliberately limited to static exponents, one would of course like to confront the theoretical predictions of [26,27] and preliminary results of [3] concerning the dynamical critical exponent z with extensive numerical simulations. Deviation from Ising universality for transitions of synchronously updated systems may here be expected on the basis of equilibrium results, where the exponent z is known to depend sharply on the type of update [38]. One would also like to learn more about the critical properties, both static and dynamic, of phase transitions of other extensively chaotic dynamical systems. Generalization to Ising-like transitions of higher-dimensional lattices is straightforward, and may lead to a numerical estimate of their upper critical dimension. Arguably, phase transitions of extended dynamical systems generically involve a broken *temporal* symmetry. Of particular interest is the case of period-doubling continuous phase transitions, whereby the macroscopic activity of lattices of, e.g., coupled logistic maps undergoes a sequence of subharmonic bifurcations [1]. Preliminary results indicate that such transitions also belong, for static critical exponents, to the universality class of Ising-like transitions of synchronously updated models [18]. The critical behavior of collective, forward Hopf bifurcations [1,43] may also yield non-mean-field critical exponents for small enough space dimensions.

Finally, we would like to make contact with real experiments, where the *methods* exposed here may be applied fruitfully, in spite of the somewhat remote nature of the models considered. Many large, homogeneous, far-from-equilibrium systems exhibit transitions between distinct spatiotemporally chaotic regimes [7,8,44], or between a (dynamically) ordered state and a spatiotemporally chaotic regime [45–47], where order parameters can be defined, and critical exponents measured. Provided that spatial coherence scales diverge at threshold, such transitions may qualify as ''continuous phase transitions,'' as defined in Sec. II A. In this case, finite-size scaling forms are expected to apply to order parameters, provided that the size L is redefined as an aspect ratio $R = L/l_0$ counted in units of the system's natural length scale l_0, as obtained from the relevant instability mechanism. When the effective system size R depends directly on one of the available control parameters, finite-size scaling may provide a feasible alternative to the (direct) measurement methods used up to now, and lead to reliable, quantitative estimates of critical exponents.

ACKNOWLEDGMENTS

We gratefully acknowledge useful discussions with Henry Greenside, Geoff Grinstein, and David Huse. Ph. M. would also like to thank Kunihiko Kaneko for his kind hospitality. This work was made possible thanks to a generous allocation of CPU time on the Cray-T3D supercomputer of Centre d'Etudes de Grenoble, Commissariat à l'Energie Atomique.

[1] H. Chaté and P. Manneville, Europhys. Lett. **17**, 291 (1992); Prog. Theor. Phys. **87**, 1 (1992); J. A. C. Gallas, P. Grassberger, H. J. Herrmann, and P. Ueberholz, Physica A **180**, 19 (1992).

[2] H. Sakaguchi, Prog. Theor. Phys. **80**, 7 (1992); Phys. Lett. A **180**, 235 (1993).

[3] J. Miller and D. Huse, Phys. Rev. E **48**, 2528 (1993).

[4] C. S. O'Hern, D. A. Egolf, and H. S. Greenside, Phys. Rev. E **53**, 3374 (1996).

[5] P. Marcq, H. Chaté, and P. Manneville, Phys. Rev. Lett. **77**, 4003 (1996).

[6] B. I. Shraiman, A. Pumir, W. Van Saarloos, P. C. Hohenberg, H. Chaté, and M. Holen, Physica D **57**, 241 (1992); D. A. Egolf and H. S. Greenside, Phys. Rev. Lett. **74**, 1751 (1995); P. Manneville and H. Chaté, Physica D **96**, 30 (1996); R. Montagne, E. Hernandez-Garcia, and M. San Miguel, Phys. Rev. Lett. **77**, 267 (1996); A. Torcini, *ibid.* **77**, 1047 (1996); A. Torcini, H. Frauenkron, and P. Grassberger (unpublished).

[7] Y. Hu, R. E. Ecke, and G. Ahlers, Phys. Rev. Lett. **74**, 394 (1995); S.W. Morris, E. Bodenshatz, D.S. Cannell, and G. Ahlers, Physica D **97**, 164 (1996).

[8] S. Kai and W. Zimmermann, Prog. Theor. Phys. Suppl. **89**, 458 (1989).

[9] D. Ruelle, Commun. Math. Phys. **87**, 287 (1982); P. Manneville, in *Macroscopic Modeling of Turbulent Flows*, edited by O. Pironneau, Lecture Notes in Physics, Vol. 230 (Springer-Verlag, New York, 1985).

[10] B. I. Shraiman and P. C. Hohenberg, Physica D **37**, 109 (1989).

[11] M. S. Bourzutschky and M. C. Cross, Chaos **2**, 173 (1992).

[12] H. Chaté and P. Manneville, Physica D **32**, 409 (1988); and in *Turbulence. A Tentative Dictionary*, edited by P. Tabeling and O. Cardoso (Plenum, New York, 1994).

[13] P. Grassberger and T. Schreiber, Physica D **50**, 177 (1991).

[14] J. M. Houlrik, I. Webman, and M. H. Jensen, Phys. Rev. A **41**, 4210 (1990); J. M. Houlrik and M. H. Jensen, Phys. Lett. A **163**, 275 (1992).
[15] Y. Kuramoto, *Chemical Oscillations, Waves, and Turbulence* (Springer-Verlag, New York, 1984); M. C. Cross and P. C. Hohenberg, Rev. Mod. Phys. **65**, 851 (1993), and references therein.
[16] L. Brunnet, H. Chaté, and P. Manneville, Physica D **78**, 141 (1994).
[17] See, e.g., Chaos **2**, 3 (1992); *Coupled Map Lattices: Theory and Experiments*, edited by K. Kaneko (World Scientific, Singapore, 1993), and references therein.
[18] H. Chaté, A. Lemaître, P. Marcq, and P. Manneville, Physica A **224**, 447 (1996); P. Marcq, H. Chaté, and P. Manneville (unpublished).
[19] See, e.g., L. A. Bunimovich and Ya G. Sinai, Nonlinearity **1**, 491 (1988); J. Bricmont and A. Kupiainen, *ibid.* **8**, 379 (1995); M. Jiang, *ibid.* **8**, 631 (1995).
[20] See, e.g., P. Chossat and M. Golubitsky, Physica D **32**, 423 (1988).
[21] H. Chaté and J. Losson (unpublished).
[22] A. Lemaître, H. Chaté, and P. Manneville, Phys. Rev. Lett. **77**, 486 (1996).
[23] See, e.g., J. Zinn-Justin, *Quantum Field Theory and Critical Phenomena* (Oxford University Press, Oxford, 1989).
[24] B. Schmittmann and R. K. P. Zia, in *Statistical Mechanics of Driven Diffusive Systems*, edited by C. Domb and J.L. Lebowitz, Phase Transitions and Critical Phenomena Vol. XVII (Academic, New York, 1995).
[25] P. C. Martin, E. D. Siggia, and H. H. Rose, Phys. Rev. A **8**, 423 (1973).
[26] G. Grinstein, C. Jayaprakash, and Y. He, Phys. Rev. Lett. **55**, 2527 (1985); T. Bohr, G. Grinstein, Y. He, and C. Jayaprakash, *ibid.* **58**, 2155 (1987).
[27] K. Bassler and B. Schmittmann, Phys. Rev. Lett. **73**, 3343 (1994).
[28] C. H. Bennett, G. Grinstein, Y. He, C. Jayaprakash, and D. Mukamel, Phys. Rev. A **41**, 1932 (1990); H. Chaté, G. Grinstein, and L.-H. Tang, Phys. Rev. Lett **74**, 912 (1995).
[29] V. Yakhot, Phys. Rev. A **24**, 642 (1981); S. Zaleski, Physica D **34**, 427 (1989).
[30] C. Boldrighini, L. A. Bunimovich, G. Cosimi, S. Frigio, and A. Pellegrinotti, J. Stat. Phys. **80**, 1185 (1995).
[31] K. Kaneko, Physica D **34**, 1 (1989); **37**, 60 (1989).
[32] *Finite-Size Scaling and Numerical Simulation of Statistical Systems*, edited by V. Privman (World Scientific, Singapore, 1990).
[33] M. E. Fisher, in *Critical Phenomena*, edited by M. S. Green (Academic, New York, 1971); M. E. Fisher and M. N. Barber, Phys. Rev. Lett. **28**, 1516 (1972).
[34] K. Binder, Z. Phys. B **43**, 119 (1980).
[35] V. Privman, P. C. Hohenberg and A. Aharony, in *Universal Critical-Point Amplitude Relations*, edited by C. Domb and J. L. Lebowitz, Phase Transitions and Critical Phenomena Vol. XIV (Academic, New York, 1991).
[36] P. Marcq, Ph. D. thesis, Université Pierre et Marie Curie, Paris, 1996.
[37] E. Medina, T. Hwa, M. Kardar, and Y.-C. Zhang, Phys. Rev. A **39**, 3053 (1989); see also T. Halpin-Healy and Y.-C. Zhang, Phys. Rep. **254**, 215 (1995) for a review.
[38] R. H. Swendsen and J. S. Wang, Phys. Rev. Lett. **58**, 86 (1987).
[39] G. Vichniac, Physica D **10**, 96 (1984).
[40] M. Suzuki, Prog. Theor. Phys. **51**, 1992 (1974).
[41] R. J. Baxter, Phys. Rev. Lett. **26**, 832 (1971); *Exactly Solved Models in Statistical Mechanics* (Academic, London, 1982).
[42] L. P. Kadanoff and F. J. Wegner, Phys. Rev. B **4**, 3989 (1971).
[43] H. Sakaguchi, Phys. Lett. A **180**, 235 (1993).
[44] T. Leweke and M. Provansal, Phys. Rev. Lett. **72**, 3174 (1994).
[45] N. B. Tufillaro, R. Ramshankar, and J. P. Gollub, Phys. Rev. Lett. **62**, 422 (1989); A. Kudrolli and J. P. Gollub, Physica D **97**, 133 (1996).
[46] Y. Hu, R. E. Ecke, and G. Ahlers, Phys. Rev. Lett. **74**, 5040 (1995).
[47] H.-W. Xu, X.-J. Li, and J. D. Gunton (unpublished).